

The system dynamics analysis, resilient and fault-tolerant control for cyber-physical systems

Linlin Li, *Senior Member, IEEE*, Steven X. Ding, Liutao Zhou, Maiying Zhong, and Kaixiang Peng

Abstract—This paper is concerned with the detection, resilient and fault-tolerant control issues for cyber-physical systems. To this end, the impairment of system dynamics caused by the defined types of cyber-attacks and process faults is analyzed. Then, the relation of the system input and output signals with the residual subspaces spanned by both the process and the controller is studied. Considering the limit capacity of standard observer-based detection and feedback control schemes in detecting and handling the cyber-attacks, a modified configuration for cyber-physical systems is developed by transmitting the combinations of the input and output residuals instead of the input and output signals, which is facile for dealing with both the process faults and cyber-attacks. It is followed by the integrated design of fault and attack detection, resilient and fault-tolerant control schemes. To enhance the detectability of cyber-attacks, the potential stealthy attack mechanisms on deteriorating the tracking behavior and feedback control performance are developed from the attackers' point of view, and the associated detection schemes for such stealthy attacks are proposed from the defenders' point of view. A case study on the robotino system is utilized to demonstrate the proposed resilient cyber-physical configuration.

Index Terms—Attack detection, fault detection, fault-tolerant control, resilient control, residual subspaces

I. INTRODUCTION

TODAY'S automatic control systems as the centrepiece of industrial cyber-physical systems (CPSs) are fully equipped with intelligent sensors, actuators and an excellent information infrastructure. It is a logic consequence of ever increasing demands for system performance and production efficiency that today's automatic control systems are of an extremely high degree of integration, automation and complexity [1]. Maintaining reliable and safe operations of automatic control systems are of elemental importance for optimally managing industrial CPSs over the whole operation life-cycle. As an indispensable maintenance functionality, real-time monitoring, fault detection (FD) and fault-tolerant control (FTC) are widely integrated in automatic control systems and runs parallel to the embedded control systems [2]–[4]. In a traditional automatic control system, FD and FTC were mainly dedicated to maintaining functionalities of sensors and actuators

as the key components embedded in the system with technical faults [1], [5].

Recently, a new type of malfunctions, the so-called cyber-attacks on automatic control systems, have drawn attention on the urgent need for developing new monitoring, diagnosis and resilient control strategies [6]–[9]. Cyber-attacks can not only considerably affect functionalities of sensors and actuators, but also impair communications among the system components and sub-systems. Different from technical faults, cyber-attacks are artificially created and could be designed by attackers in such a way that they cannot be detected using the existing diagnosis techniques and lead to immense damages during system operations [10], [11]. Such cyber-attacks are called stealthy. A further type of cyber-attacks are the so-called eavesdropping attacks [12]. Although such attacks do not cause changes in system dynamics and performance degradation, they enable adversary to gain system knowledge which can be used to design, for instance, stealthy attacks [11], [13]–[15]. As a result, an early and reliable detection of cyber-attacks is becoming a vital requirement on cyber-security of industrial CPSs [16]. In the literature, a great number of results have been reported about detecting the so-called replay, zero dynamics, covert attacks, false data injection attacks or kernel attacks, which are stealthy integrity attacks and cannot, structurally, be detected by means of a standard observer-based fault detection system [7], [12], [17]. Specifically, alternative detection schemes have been proposed for the detection of stealthy integrity attacks in the so-called unified control and detection framework [17]. By extending the residual detection to both the system input and output subspaces, the stealthy attack can be well detected. On the other hand, innumerable capable diagnosis of both the physical faults and attacks have been developed with various specifications in recent years [18]–[20]. To our best knowledge, limit attention has been made on the analysis of the influence of the physical faults and attacks on the systems dynamics and distinguish them structurally.

As a response to the security issues of CPSs, resilient control has received increasing attention from both the research and application domains. As appropriate control-theoretic countermeasures, the so-called resource-aware secure control methods [6], like event-triggered control algorithms or switching control mechanisms, are prevalent resilient control schemes. Roughly speaking, these methods make the CPSs highly resilient against attacks by means of optimal management of data communications among subsystems in the CPS. On the other hand, the well-established control techniques have been widely implemented in resilient control, for instance model predictive control [21], adaptive control [22], and sliding mode

This work has been supported by the National Natural Science Foundation of China under Grants 62322303, 62233012, and U21A20483.

L. Li and K. Peng are with School of Automation and Electrical Engineering, University of Science and Technology Beijing, Beijing 100083, P. R. China. Email: linlin.li@ustb.edu.cn, kaixiang@ustb.edu.cn.

S. X. Ding and L. Zhou are with the Institute for Automatic Control and Complex Systems (AKS), University of Duisburg-Essen, Germany. Email: steven.ding@uni-due.de, liutao.zhou@uni-due.de.

M. Zhong is with the College of Electrical Engineering and Automation, Shandong University of Science and Technology, Qingdao 266590, China. Email: mzhong@buaa.edu.cn.

control [23]. Most of the existing methods require the precise information of the states of CPSs. To this end, the resilient state estimation has been studied by applying the Kalman filter, Luenberger observer and extended state observer as the tools [6], which dominates the thematic area of resilient control of CPSs. An immediate consequence is that the proposed design algorithms for resilient control are limited to updating the existing methods and schemes for FTC [24]. In recent years, the integrated design of FD and FTC is state of the art of the advanced FTC technique. Reviewing the recent publications shows that most of the studies on resilient control of CPSs address detection, estimation and control issues separately. Our work is motivated by the above observation and in particular driven by the question: What is difference of the impact on the system dynamics for cyber-attacks and technical faults? What is the difference between FD and attack detection, and further FTC and resilient control? Is it possible to develop an alternative CPS configuration to achieve the detection, resilient and FTC for both the cyber-attacks and technical faults in the integrated fashion?

In the recent decade, a trend of investigating attack mechanisms can be observed, which is not only helpful to assess the security weakness and vulnerability of CPSs, but also useful in designing the defense strategy [25], [26]. Among the involved studies, the denial-of-service (DoS) attacks [27] and deception attacks [28], as the main categories of malicious attacks, attracted the major attention. By blocking the communication links of system components over wireless networks, DoS attacks can degrade the system performance [29], [30]. The deception attacks are usually designed by the attacks to cause system performance degradation through modifying data packets without being detected. Among the involved studies, switched strategy [31], multi-sensor joint attack [32], [33], data-driven method [28], [34], built the main stream. Nevertheless, the major attention has been paid to degrade the tracking performance, enlarge the state estimation error, and increase linear quadratic Gaussian (LQG) control performance [35]–[38], while limit research efforts have been made on deteriorating the feedback control performance [39]. On the other hand, most of the existing attack design schemes are implemented based on some strict assumptions, which limits the applications.

Inspired by these observations, the main objective of this paper is to deal with the fault and cyber-security issues in a systematic and reliable manner. The main contributions can be summarized as follows:

- The systematic analysis of the closed-loop dynamics of CPSs under technical faults and defined types of cyber-attacks, and the attack- and fault-induced impairment of system dynamics are given for the first time.
- The parameterization form of the closed-loop dynamics is studied first, and the relation of system signal subspace with the residual subspaces spanned by both the input and output signal is established.
- A modified CPS configuration is developed by utilizing the combinations of the input and output residuals as the transmitted data instead of the process input and output to ensure i) the cyber-security in case that the communications fail, ii) detection of cyber-attacks and

technical faults, and iii) the data privacy.

- The integrated design scheme for fault and attack detection, FTC and resilient control is investigated for the first time based on the proposed CPS configuration.
- The stealthy attack design schemes are proposed for deteriorating the tracking behavior and feedback control performance respectively from the attackers' point of view. Then, from the defenders' point of view, two performance degradation monitoring-based detection methods of stealthy attacks are developed.

Notations. \mathcal{H}_2^m represents the signal space of all the signals of dimension m with bounded energy. \mathcal{RH}_∞ denotes the space of all rational transfer functions of stable systems. The root mean square (RMS) of signal α over the time interval $[k+1, k+\tau]$ is defined as $\|\alpha\|_{RMS,[k+1,k+\tau]} := \sqrt{\frac{1}{\tau} \sum_{i=k+1}^{k+\tau} \alpha^T(i) \alpha(i)}$.

II. PRELIMINARIES AND PROBLEM FORMULATION

A. System factorizations

Consider the following linear discrete-time system

$$\begin{aligned} x(k+1) &= Ax(k) + Bu(k) + E_f f + w(k) \\ y(k) &= Cx(k) + Du(k) + F_f f + \nu(k) \end{aligned} \quad (1)$$

where $y \in \mathcal{R}^{k_y}$, $u \in \mathcal{R}^{k_u}$, $x \in \mathcal{R}^{k_x}$ denote the output, input and state, respectively. $w(k), \nu(k)$ represent the process and measurement noise with $w \sim (0, \Sigma_w), \nu \sim (0, \Sigma_\nu)$. A, B, C, D are system matrices with appropriate dimensions. f denotes the technical fault with E_f, F_f as the distribution matrices.

Let $G = (A, B, C, D)$. $G(z) = N(z)M^{-1}(z) = \hat{M}^{-1}(z)\hat{N}(z)$ are called the right coprime factorization (RCF) and left coprime factorization (LCF) of $G(z)$ respectively if there exists $X(z), Y(z), \hat{X}(z), \hat{Y}(z) \in \mathcal{RH}_\infty$ such that the following Bezout identity holds

$$\begin{bmatrix} X(z) & Y(z) \\ -\hat{N}(z) & \hat{M}(z) \end{bmatrix} \begin{bmatrix} M(z) & -\hat{Y}(z) \\ N(z) & \hat{X}(z) \end{bmatrix} = I \quad (2)$$

where $M(z), N(z), \hat{M}(z), \hat{N}(z) \in \mathcal{RH}_\infty$. The state space representations for the associated transfer matrices in Bezout identity are given by

$$\begin{aligned} \hat{M} &= (A-LC, -L, WC, W), \hat{N} = (A-LC, B-LD, WC, WD) \\ M &= (A+BF, BV, F, V), N = (A+BF, BV, C+DF, DV) \\ \hat{X} &= (A+BF, L, C+DF, W^{-1}), \hat{Y} = (A+BF, -LW^{-1}, F, 0) \\ X &= (A-LC, -(B-LD), F, I), Y = (A-LC, -L, F, 0) \end{aligned} \quad (3)$$

where F, L are selected such that $A-LC$ and $A+BF$ are Schur matrices. W and V are invertible matrices [2], [40].

According to Youla parameterization, all the controllers that can stabilize the plant $G(z)$ can be parameterized by

$$K = -(\hat{Y} - MQ)(\hat{X} + NQ)^{-1} = -(X + Q\hat{N})^{-1}(Y - Q\hat{M}) \quad (4)$$

where $Q \in \mathcal{RH}_\infty$ is the parameter system [40].

B. The signal subspaces

The input and output (I/O) signal space of the system (1) can be described by the following definition.

Definition 1. Consider the system (1) with the RCF and LCF as $G(z) = N(z)M^{-1}(z) = \hat{M}^{-1}(z)\hat{N}(z)$. The kernel and image subspaces of the system (1) are defined by

$$\mathcal{K}_G = \left\{ \begin{bmatrix} u \\ y \end{bmatrix} \in \mathcal{H}_2^{k_u+k_y} : [-\hat{N} \ \hat{M}] \begin{bmatrix} u \\ y \end{bmatrix} = 0 \right\} \quad (5)$$

$$\mathcal{I}_G = \left\{ \begin{bmatrix} u \\ y \end{bmatrix} \in \mathcal{H}_2^{k_u+k_y} : \begin{bmatrix} u \\ y \end{bmatrix} = \begin{bmatrix} M \\ N \end{bmatrix} v, v \in \mathcal{H}_2^{k_u} \right\}. \quad (6)$$

It is well known that the LCF can be applied as the residual generator which is essential in fault detection

$$r_y(z) = -\hat{N}(z)u(z) + \hat{M}(z)y(z) \quad (7)$$

where r_y represents the residual signal delivering the information for the uncertainties and potential faults. The state-space representation can be written into the observer-based form

$$\begin{aligned} \hat{x}(k+1) &= A\hat{x}(k) + Bu(k) + LW^{-1}r_y(k) \\ r_y(k) &= W(y(k) - \hat{y}(k)), \hat{y}(k) = C\hat{x}(k) + Du(k) \end{aligned} \quad (8)$$

where \hat{x}, \hat{y} denotes the state and output estimation, respectively.

Recall that due to Bezout identity,

$$\forall \begin{bmatrix} u \\ y \end{bmatrix} \in \mathcal{I}_G, r_y = [-\hat{N} \ \hat{M}] \begin{bmatrix} u \\ y \end{bmatrix} = 0.$$

It is of interest to notice that the residual $r_y \neq 0$ delivers the information for the potential uncertainties and faults in the process. On the basis of the Bezout identity, it turns out

$$\forall r_y \neq 0, r_y(z) = \begin{bmatrix} -\hat{Y}(z) + M(z)Q(z) \\ \hat{X}(z) + N(z)Q(z) \end{bmatrix} r_y(z).$$

Recall that $(\hat{X}(z) + N(z)Q(z), -\hat{Y}(z) + M(z)Q(z))$ build the LCF of the controller $K(z)$. Consequently, any process I/O data which ensures $r_y \neq 0$ can be characterized by the image subspace of the controller.

Definition 2. The image subspace of controller (4) is given by

$$\mathcal{I}_K = \left\{ \begin{bmatrix} u \\ y \end{bmatrix} \in \mathcal{H}_2^{k_u+k_y}, \begin{bmatrix} u \\ y \end{bmatrix} = \begin{bmatrix} -\hat{Y} + MQ \\ \hat{X} + NQ \end{bmatrix} r_y, r_y \in \mathcal{H}_2^{k_y} \right\}.$$

C. Problem formulation

With rapidly increasing threats of cyber-crime and the resulted damages to industrial CPSs, cyber-security imposes new challenging issues in research of diagnosis and resilient control of both cyber-attacks and technical faults, which should be managed with high reliability and in an integrated fashion with the existing control and monitoring algorithms and facilities. Thus, the main objective of this paper is to develop a detection, resilient and fault-tolerant control framework in a systematic and reliable manner. To this end, our efforts in the first part of this paper have been mainly made on

- analyzing the attack- and fault-induced impairment of system dynamics of a general type of CPSs, and
- discussing the potential of the existing control and detection methods to manage the system performance impairment due to the cyber-attacks and technical faults.

It can be shown that the standard observer-based detection and feedback control schemes are limited in dealing with cyber-attacks. Thus, it is the main objective of the second part of this paper to develop a modified CPS configuration which guarantee

not only high resilience of CPSs under cyber-attacks and high fault tolerance against process faults, but also ensure ‘‘fail-safe’’ cyber-security and data privacy. Then the integrated design schemes for i) fault detection, ii) attack detection, iii) resilient and fault-tolerant control are studied. To further enhance the security of the CPSs, the stealthy attack design schemes are proposed for deteriorating the tracking behavior and feedback control performance respectively from the attackers’ point of view. Then, from the defenders’ point of view, the associated performance degradation monitoring-based detection methods of stealthy attacks are developed.

III. ANALYSIS OF SYSTEM DYNAMICS UNDER CYBER-ATTACKS AND FAULTS

In this section, the system dynamics under cyber-attacks and faults for a general type of CPS systems are analyzed.

Consider a CPS system modelled by (1). The control signal u_{MC} is generated at the control station as

$$u_{MC}(z) = K(z)y^a(z) + v(z) \quad (9)$$

and sent to the plant as $u(z) = u_{MC}^a(z)$ with the following general type of cyber-attacks under consideration

$$y^a(k) = y(k) + a_y(k), u_{MC}^a(k) = u_{MC}(k) + a_{u_{MC}}(k) \quad (10)$$

where a_y and $a_{u_{MC}}$ represent the cyber-attacks injected into the output and input communication channels, respectively. $K(z)$ is the feedback gain matrix given by (4) and $v(z)$ denotes the reference signal.

A. Impairment of system dynamics caused by cyber-attacks and faults

We now analyze the possible impairment of the system dynamics under the faults and the cyber-attacks (10). To ease the presentation, an alternative representation of the plant (1) is studied first.

Theorem 1. The process (1) can be equivalently described by

$$y(z) = G(z)u(z) + \hat{M}^{-1}(z)r_y(z) \quad (11)$$

with $r_y(z)$ generated by (8).

Proof. It is evident that the process (1) can be described by the following kernel-based system I/O model [1]

$$y(k) = \hat{y}(k) + W^{-1}r_y(k). \quad (12)$$

Observe that this model can be equivalently written into

$$y(z) = G(z)u(z) + \left(I + (zI - A)^{-1}L \right) W^{-1}r_y(z).$$

It is of interest to notice that

$$\left(I + (zI - A)^{-1}L \right) W^{-1} = \hat{M}^{-1}(z)$$

which completes the proof. \square

Remark 1. It is noteworthy that the kernel-based system I/O-model (11) describes the system dynamics without approximation, independent of the existence of any type of uncertainties and plant faults. Thus, throughout of the paper, (11) is adopted to represent the process (1).

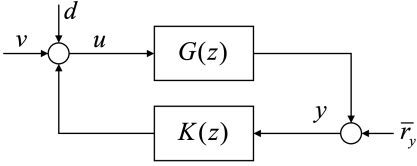


Fig. 1. The equivalent system dynamics for CPS systems with cyber-attacks

Theorem 2. *Given CPS modelled by (9)-(11), the system dynamics under the attacks and faults are governed by*

$$\begin{bmatrix} u \\ y \end{bmatrix} = \begin{bmatrix} M \\ N \end{bmatrix} (\bar{v} + d_a) + \begin{bmatrix} -\hat{Y} + MQ \\ \hat{X} + NQ \end{bmatrix} r_y, \quad (13)$$

$$\bar{v} = (X + Q\hat{N})v, d_a = (X + Q\hat{N})a_{u_{MC}} - (Y - Q\hat{M})a_y.$$

Proof. It is straightforward that

$$u = u_{MC} + a_{u_{MC}} = Ky + v + d, d = Ka_y + a_{u_{MC}}. \quad (14)$$

Considering the process model (11) and (14), together with the coprime factorization of G, K , it is easy to see

$$\begin{aligned} \begin{bmatrix} u \\ y \end{bmatrix} &= \begin{bmatrix} I & -K \\ -G & I \end{bmatrix}^{-1} \begin{bmatrix} v + d \\ \hat{M}^{-1}r_y \end{bmatrix} \\ &= \begin{bmatrix} X + Q\hat{N} & Y - Q\hat{M} \\ -\hat{N} & \hat{M} \end{bmatrix}^{-1} \begin{bmatrix} (X + Q\hat{N})(v + d) \\ r_y \end{bmatrix} \\ &= \begin{bmatrix} M & -\hat{Y} + MQ \\ N & \hat{X} + NQ \end{bmatrix} \begin{bmatrix} (X + Q\hat{N})(v + d) \\ r_y \end{bmatrix} \end{aligned}$$

which completes the proof. \square

According to (14), the equivalent configuration of the CPS under cyber-attacks is depicted in Fig. 6 with $\bar{r}_y = \hat{M}^{-1}r_y$. It is of interest to notice that the impacts of the cyber-attacks on the closed-loop dynamics are equivalently modelled as an unknown input added to the reference signal.

In what follows, we further analyze the system dynamics under the cyber-attacks a_y and $a_{u_{MC}}$ modelled by

$$\begin{bmatrix} a_{u_{MC}}(z) \\ a_y(z) \end{bmatrix} = \Pi^a(z) \begin{bmatrix} u_{MC}(z) \\ y(z) \end{bmatrix} + \begin{bmatrix} \epsilon_u(z) \\ \epsilon_y(z) \end{bmatrix} \quad (15)$$

where Π^a is a stable dynamic system with (u_{MC}, y) as the input variables. ϵ_u and ϵ_y are \mathcal{L}_2 -bounded, unknown, and assumed to be independent of u, y , which can be considered as the additive attacks. $\Pi^a(z) \begin{bmatrix} u_{MC}(z) \\ y(z) \end{bmatrix}$ is adopted to model the possible cyber-attacks which are designed and artificially designed by attackers in possession of data (u_{MC}, y) , which can be interpreted as multiplicative attacks.

Here, without loss of generality, it is assumed that $\bar{\Pi}^a = I + \begin{bmatrix} I & 0 \\ 0 & 0 \end{bmatrix} \Pi^a$ is invertible.

Theorem 3. *Given the CPS system (9)-(11), the system dynamics under the cyber-attacks (15) are governed by*

$$\begin{aligned} \begin{bmatrix} u \\ y \end{bmatrix} &= \begin{bmatrix} M \\ N \end{bmatrix} \bar{v} + \begin{bmatrix} -\hat{Y} + MQ \\ \hat{X} + NQ \end{bmatrix} r_y \\ &- \begin{bmatrix} M \\ N \end{bmatrix} \left(I + \Phi \begin{bmatrix} M \\ N \end{bmatrix} \right)^{-1} \Phi \begin{bmatrix} M \\ N \end{bmatrix} \bar{v} \end{aligned}$$

$$\begin{aligned} &- \begin{bmatrix} M \\ N \end{bmatrix} \left(I + \Phi \begin{bmatrix} M \\ N \end{bmatrix} \right)^{-1} \Phi \begin{bmatrix} -\hat{Y} + MQ \\ \hat{X} + NQ \end{bmatrix} r_y \\ &+ \begin{bmatrix} M \\ N \end{bmatrix} \left(I + \Phi \begin{bmatrix} M \\ N \end{bmatrix} \right)^{-1} \Psi \begin{bmatrix} \epsilon_u \\ \epsilon_y \end{bmatrix} \end{aligned} \quad (16)$$

where

$$\begin{aligned} \Phi &= -[X + Q\hat{N} \quad -Y + Q\hat{M}] \Pi^a (\bar{\Pi}^a)^{-1} \\ \Psi &= [X + Q\hat{N} \quad -Y + Q\hat{M}] - \Phi \begin{bmatrix} -I & 0 \\ 0 & 0 \end{bmatrix}, \bar{v} = (X + Q\hat{N})v. \end{aligned}$$

Moreover, the CPS dynamic can be equivalently expressed by

$$\begin{cases} y = Gu + \hat{M}^{-1}r_y \\ u = K_\Delta y + \Delta_{\bar{v}} + d, \end{cases} \quad (17)$$

$$\Delta_{\bar{v}} = (X + Q\hat{N} + \Delta K_u)^{-1} \bar{v}, d = (X + Q\hat{N} + \Delta K_u)^{-1} \Psi \begin{bmatrix} \epsilon_u \\ \epsilon_y \end{bmatrix}$$

$$K_\Delta = -(X + Q\hat{N} + \Delta K_u)^{-1} (Y - Q\hat{M} + \Delta K_y),$$

$$\Delta K_u = \Phi(:, 1 : k_u), \Delta K_y = \Phi(:, k_u + 1 : k_u + k_y).$$

Proof. It follows from the proof of Theorem 2 that the system dynamics can be described by

$$\begin{aligned} \begin{bmatrix} u \\ y \end{bmatrix} &= \begin{bmatrix} M \\ N \end{bmatrix} \left(\bar{v} + [X + Q\hat{N} \quad -Y + Q\hat{M}] \left(\Pi^a \begin{bmatrix} u_{MC} \\ y \end{bmatrix} + \begin{bmatrix} \epsilon_u \\ \epsilon_y \end{bmatrix} \right) \right) \\ &+ \begin{bmatrix} -\hat{Y} + MQ \\ \hat{X} + NQ \end{bmatrix} r_y. \end{aligned}$$

Observe that

$$\begin{aligned} \begin{bmatrix} u_{MC} \\ y \end{bmatrix} &= \begin{bmatrix} u \\ y \end{bmatrix} + \begin{bmatrix} -I & 0 \\ 0 & 0 \end{bmatrix} \left(\Pi^a \begin{bmatrix} u_{MC} \\ y \end{bmatrix} + \begin{bmatrix} \epsilon_u \\ \epsilon_y \end{bmatrix} \right) \\ &= \left(I + \begin{bmatrix} I & 0 \\ 0 & 0 \end{bmatrix} \Pi^a \right)^{-1} \begin{bmatrix} u \\ y \end{bmatrix} + \left(I + \begin{bmatrix} I & 0 \\ 0 & 0 \end{bmatrix} \Pi^a \right)^{-1} \begin{bmatrix} -I & 0 \\ 0 & 0 \end{bmatrix} \begin{bmatrix} \epsilon_u \\ \epsilon_y \end{bmatrix} \end{aligned}$$

which yields

$$\begin{aligned} \begin{bmatrix} u \\ y \end{bmatrix} &= \begin{bmatrix} M \\ N \end{bmatrix} \left(\bar{v} - \Phi \begin{bmatrix} u \\ y \end{bmatrix} + \Psi \begin{bmatrix} \epsilon_u \\ \epsilon_y \end{bmatrix} \right) + \begin{bmatrix} -\hat{Y} + MQ \\ \hat{X} + NQ \end{bmatrix} r_y \\ &= \left(I + \begin{bmatrix} M \\ N \end{bmatrix} \Phi \right)^{-1} \left(\begin{bmatrix} M \\ N \end{bmatrix} \left(\bar{v} + \Psi \begin{bmatrix} \epsilon_u \\ \epsilon_y \end{bmatrix} \right) + \begin{bmatrix} -\hat{Y} + MQ \\ \hat{X} + NQ \end{bmatrix} r_y \right). \end{aligned}$$

After some routine calculations using the relation

$$\left(I + \begin{bmatrix} M \\ N \end{bmatrix} \Phi \right)^{-1} = I - \begin{bmatrix} M \\ N \end{bmatrix} \left(I + \Phi \begin{bmatrix} M \\ N \end{bmatrix} \right)^{-1} \Phi,$$

we have (16). Noticing that

$$\begin{aligned} u &= Ky^a + v + a_{u_{MC}} = Ky + Ka_y + v + a_{u_{MC}} \implies \\ (X + Q\hat{N})u &= (-Y + Q\hat{M})(y + a_y) + (X + Q\hat{N})(v + a_{u_{MC}}) \\ &= (-Y + Q\hat{M})y + (X + Q\hat{N})v - \Phi \begin{bmatrix} u \\ y \end{bmatrix} + \Psi \begin{bmatrix} \epsilon_u \\ \epsilon_y \end{bmatrix}, \end{aligned}$$

(17) is finally proved. \square

It follows from (16) in Theorem 3 that the system dynamics consists of five terms. The first two terms give the nominal system response (attack-free dynamic), while the third and fourth terms describe the deviations caused by the cyber-attacks modelled by (15) in the responses to the reference signal and to the plant residual, respectively. The fifth term gives the deviations caused by the additive cyber-attacks ϵ_u, ϵ_y .

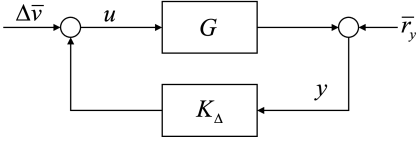


Fig. 2. The equivalent system dynamics for CPS systems with multiplicative cyber-attacks

When $\epsilon_u = 0, \epsilon_y = 0$, $a_y, a_{u_{MC}}$ can be interpreted as the multiplicative cyber-attacks. The equivalent configuration of the CPS closed-loop dynamic under multiplicative cyber-attacks is sketched in Fig. 7. It is evident that the uncertainty in the feedback controller in case of the multiplicative attacks, may affect the loop stability and feedback performance.

Remark 2. *It is worth mentioning that the additive cyber-attacks (10) deviate the system response to the reference signal from the nominal value, while the multiplicative cyber-attacks (15) lead to the change both to the reference response and feedback control performance.*

B. Analysis of system dynamics under cyber-attacks and faults

On the basis of Theorems 2-3 and the Bezout identity

$$-\hat{N}M + \hat{M}N = 0 \quad (18)$$

it is evident that r_y is independent of $a_y, a_{u_{MC}}$. Thus, the following corollary is straightforward.

Corollary 1. *Given CPS modelled by (9)-(11), both the additive attacks (10) and multiplicative attacks (15), lead to variations exclusively in the system image subspace \mathcal{I}_G , while the process uncertainties and faults, reflected by the residual r_y , results in change solely in the controller image subspace \mathcal{I}_K .*

It is apparent that the residual generator, $r_y = \hat{M}y - \hat{N}u$, embedded and implemented at the plant side only reflects the uncertainties and faults in the residual subspace, and thus can not detect the cyber-attacks. In addition, the following claims are of considerable importance:

- detection and control of CPSs under cyber-attacks and dynamic processes suffering uncertainties or faults are two different but dual problems. This conclusion illustrates that the common view of considering distinguishing/isolating cyber-attacks and process faults as a challenging issue, because of their similar forms, is less convincing,
- instead, the real challenges are the development of novel detection and (feedback) control schemes that are capable to detect and control the uncertainties in the plant image subspace. It is known that the traditional detection and control methods are dedicated to handling the uncertainties and faults in the plant. Since those uncertainties, including unknown inputs and faults, are indeed uncertainties in the controller image subspace, which is a complement of the system image subspace, the traditional methods are less (or even not) capable to detect and control of cyber-attacks, and

- concretely, methods should be developed to detect and control of cyber-attacks in the plant image subspace.

The above observations motivate us to find an alternative solution for the integrated design of detection and resilient control of both technical faults and cyber-attacks for CPSs in the subsequent sections.

IV. ALTERNATIVE REPRESENTATION OF PROCESS SIGNAL

The fact that the output residual r_y cannot detect and control cyber-attacks implies that additional information about the CPS dynamics is needed. Intuitively, informations related to the input residual is an immediate candidate. This motivates us to define the input residual r_u on the plant side as

$$r_u(z) := (X(z) + Q(z)\hat{M}(z))u(z) + (Y(z) - Q(z)\hat{M}(z))y(z) \quad (19)$$

Substituting (13) into (19) leads to

$$r_u(z) := \bar{v} + (X + Q\hat{N})a_{u_{MC}} - (Y - Q\hat{M})a_y. \quad (20)$$

It is evident that r_u is a natural information provider of the cyber-attacks ($a_y, a_{u_{MC}}$). In this section, the role of r_u in the closed-loop dynamics is further examined, which lays the foundation for the subsequent study.

A. The parameterization of closed-loop dynamics

Without loss of generality, we consider the process (11) with the controller $u(z) = -X^{-1}(z)Y(z)y(z) + v(z)$. It follows from the previous discussions that the process can be equivalently described by

$$\begin{cases} \hat{x}(k+1) = (A + BF)\hat{x}(k) + Br_u(k) + Lr_y(k) \\ y(k) = C\hat{x}(k) + Du(k) + r_y(k) \\ u(k) = F\hat{x}(k) + \bar{v}(k), \bar{v}(z) = X(z)v(z) \\ r_y(k) = y(k) - C\hat{x}(k) - Du(k) \end{cases} \quad (21)$$

where

$$r_u(z) := X(z)u(z) + Y(z)y(z) = u(z) - F\hat{x}(z). \quad (22)$$

It is noteworthy that the selection of F, L has no influence on the transfer function $G(z)$. That is, $G(z)$ is invariant to F, L . Consequently, we have the following theorem.

Theorem 4. *Given $F_i \neq F, L_i \neq L, i = 1, \dots, \kappa$ which ensures that $A_{F_i} = A + BF_i$ is Schure, (21) can be equivalently realized by*

$$\begin{cases} \hat{x}(k+1) = A_{F_i}\hat{x}(k) + Br_{u,i}(k) + L_i r_{y,i}(k) \\ u(k) = F_i\hat{x}(k) + r_{Q_i}(k) + \bar{v}_i(k), \bar{v}_i(z) = (X_i(z) + Q_i(z)\hat{N}_i(z))v(z) \\ r_{Q_i}(z) = M_i(z)Q_i(z)r_{y,i}(z) \\ y(k) = C\hat{x}(k) + Du(k) + r_{y,i}(k) \end{cases}$$

where $X_i, Y_i, M_i, N_i, \hat{X}_i, \hat{Y}_i, \hat{N}_i, \hat{M}_i$ are transfer functions given by (3) with $F = F_i, L = L_i$, and

$$r_{u,i}(z) := X_i(z)u(z) + Y_i(z)y(z) = u(z) - F_i\hat{x}(z)$$

$$r_{y,i}(z) = -\hat{N}_i(z)u(z) + \hat{M}_i(z)y(z) = y(z) - C\hat{x}(z) - Du(z)$$

$$\bar{V}_{i0} = [X \ Y] \begin{bmatrix} -\hat{Y}_i \\ \hat{X}_i \end{bmatrix}, \bar{R}_{i0} = [X_i \ Y_i] \begin{bmatrix} -\hat{Y}_i \\ \hat{X}_i \end{bmatrix}$$

$$V_{i0} = I + (F_i - F)(zI - A_{F_i})^{-1}B, Q_i(z) = \bar{R}_{i0}(z)R_{0i}(z)$$

$$R_{0i} = I - C(zI - A_L)^{-1}(L - L_i), r_{Q_i}(z) = Q_i(z)r_{y,i}(z).$$

Proof. It is straightforward that

$$u(k) = F\hat{x} + \bar{v} = -\hat{Y}r_y + M\bar{v}. \quad (23)$$

By means of Bezout identity (2), $\begin{bmatrix} X & Y \\ \hat{X} & \hat{X} \end{bmatrix}$ can be parameterized respectively by

$$\begin{bmatrix} -\hat{Y} \\ \hat{X} \end{bmatrix} = \begin{bmatrix} M_i & -\hat{Y}_i \\ N_i & \hat{X}_i \end{bmatrix} \begin{bmatrix} Q_{1i} \\ Q_{2i} \end{bmatrix}, \begin{bmatrix} X & Y \\ \hat{X} & \hat{X} \end{bmatrix} = \begin{bmatrix} \bar{Q}_{1i} & \bar{Q}_{2i} \end{bmatrix} \begin{bmatrix} X_i & Y_i \\ -\hat{N}_i & \hat{M}_i \end{bmatrix}$$

for some $Q_{1i}, Q_{2i}, \bar{Q}_{1i}, \bar{Q}_{2i} \in \mathcal{RH}_\infty$. It follows from [1] that

$$\begin{bmatrix} -\hat{N}_i & \hat{M}_i \end{bmatrix} = R_{i0} \begin{bmatrix} -\hat{N} & \hat{M} \end{bmatrix}, \begin{bmatrix} M_i \\ N_i \end{bmatrix} = \begin{bmatrix} M \\ N \end{bmatrix} V_{i0}$$

and $R_{i0}^{-1} = R_{0i}, V_{i0}^{-1} = V_{0i}$. Consequently, we have

$$\begin{bmatrix} -\hat{N} & \hat{M} \end{bmatrix} \begin{bmatrix} -\hat{Y} \\ \hat{X} \end{bmatrix} = R_{0i} \begin{bmatrix} -\hat{N}_i & \hat{M}_i \end{bmatrix} \begin{bmatrix} M_i & -\hat{Y}_i \\ N_i & \hat{X}_i \end{bmatrix} \begin{bmatrix} Q_{1i} \\ Q_{2i} \end{bmatrix} = R_{0i} Q_{2i} = I$$

$$\begin{bmatrix} X & Y \\ \hat{X} & \hat{X} \end{bmatrix} \begin{bmatrix} M \\ N \end{bmatrix} = \begin{bmatrix} \bar{Q}_{1i} & \bar{Q}_{2i} \end{bmatrix} \begin{bmatrix} X_i & Y_i \\ -\hat{N}_i & \hat{M}_i \end{bmatrix} \begin{bmatrix} M_i \\ N_i \end{bmatrix} V_{0i} = \bar{Q}_{1i} V_{0i} = I$$

Moreover, it is evident that

$$V_{i0} = \begin{bmatrix} X & Y \\ \hat{X} & \hat{X} \end{bmatrix} \begin{bmatrix} -\hat{Y}_i \\ \hat{X}_i \end{bmatrix} = \begin{bmatrix} \bar{Q}_{1i} & \bar{Q}_{2i} \end{bmatrix} \begin{bmatrix} X_i & Y_i \\ -\hat{N}_i & \hat{M}_i \end{bmatrix} \begin{bmatrix} -\hat{Y}_i \\ \hat{X}_i \end{bmatrix} = \bar{Q}_{2i}$$

$$\bar{R}_{i0} = \begin{bmatrix} X_i & Y_i \end{bmatrix} \begin{bmatrix} -\hat{Y}_i \\ \hat{X}_i \end{bmatrix} = \begin{bmatrix} X_i & Y_i \end{bmatrix} \begin{bmatrix} M_i & -\hat{Y}_i \\ N_i & \hat{X}_i \end{bmatrix} \begin{bmatrix} Q_{1i} \\ Q_{2i} \end{bmatrix} = Q_{1i}.$$

As a result, one has that

$$\begin{aligned} u &= -\hat{Y}_i R_{i0} r_y + M_i \bar{R}_{i0} r_y + M_i V_{i0} (V_{0i} X_i - \bar{V}_{i0} \hat{N}_i) v \\ &= -\hat{Y}_i r_{y,i} + M_i \bar{R}_{i0} R_{0i} r_{y,i} + M_i (X_i - V_{0i} \bar{V}_{i0} \hat{N}_i) v \\ &= F_i \hat{x} + r_{Q_i} + \bar{v}_i \end{aligned}$$

which completes the proof. \square

Remark 3. *Theorem 4 reveals that varying F, L to F_i, L_i is equivalent to adding a stable post-filter and additional residual signal to u, v without changing the process dynamics.*

The closed-loop dynamics for different setting of L_i, F_i is analyzed in the following corollary.

Corollary 2. *The closed-loop dynamics for process (21) can be equivalently described by*

$$\begin{bmatrix} u \\ y \end{bmatrix} = \begin{bmatrix} M \\ N \end{bmatrix} r_u + \begin{bmatrix} -\hat{Y} \\ \hat{X} \end{bmatrix} r_y = \begin{bmatrix} M \\ N \end{bmatrix} Q_{u_i} r_{u,i} + \begin{bmatrix} -\hat{Y} + M Q_{e_i} \\ \hat{X} + N Q_{e_i} \end{bmatrix} r_{y,i}$$

$$Q_{u_i} = V_{i0}, Q_{e_i} = \bar{V}_{i0} + \bar{R}_{i0} R_{i0}^{-1}. \quad (24)$$

Proof. It follows from the poof of Theorem 4 that the system dynamics (21) can be equivalently written as

$$\begin{bmatrix} u \\ y \end{bmatrix} = \begin{bmatrix} X & Y \\ -\hat{N} & \hat{M} \end{bmatrix}^{-1} \begin{bmatrix} r_u \\ r_y \end{bmatrix} = \begin{bmatrix} M \\ N \end{bmatrix} r_u + \begin{bmatrix} -\hat{Y} \\ \hat{X} \end{bmatrix} r_y$$

$$= \begin{bmatrix} M \\ N \end{bmatrix} (V_{i0} r_{u,i} + \bar{V}_{i0} r_{y,i}) + \left(\begin{bmatrix} -\hat{Y}_i \\ \hat{X}_i \end{bmatrix} R_{i0} + \begin{bmatrix} M_1 \\ N_1 \end{bmatrix} \bar{R}_{i0} \right) r_y.$$

On the basis of [2], we have

$$R_{i0} \begin{bmatrix} -\hat{N} & \hat{M} \end{bmatrix} = \begin{bmatrix} -\hat{N}_i & \hat{M}_i \end{bmatrix} \implies R_{i0} r_y = r_{y,i}$$

which completes the proof. \square

Remark 4. (24) can be considered as a full parameterization of CPS closed-loop dynamic with $Q_{u_i}, Q_{e_i} \in \mathcal{RH}_\infty$ as the parameter systems.

B. The process signal subspace and residual subspaces

It follows from the proof of Corollary 2 that

$$\begin{bmatrix} r_u \\ r_y \end{bmatrix} = \begin{bmatrix} X & Y \\ -\hat{N} & \hat{M} \end{bmatrix} \begin{bmatrix} u \\ y \end{bmatrix}. \quad (25)$$

It is evident that the process data (u, y) and the I/O residual signals (r_u, r_y) is one-to-one mapping. Notice that r_u, r_y build the system and controller image subspaces \mathcal{I}_G and \mathcal{I}_K , respectively, which are complementary. Consequently, we have the following lemma.

Lemma 1. *The system signal space*

$$\mathcal{S} = \left\{ \begin{bmatrix} u \\ y \end{bmatrix} \in \mathcal{H}_2^{k_u + k_y} \right\} \quad (26)$$

with u, y as the input and output of the process (1), can be constructed by

$$\mathcal{S} = \mathcal{I}_G \oplus \mathcal{I}_K. \quad (27)$$

Remark 5. *To summarize, the system I/O signal consists of the process image and controller image subspaces. The image subspace of the process is driven by r_u , which describes the response of I/O signal to the reference and cyber-attacks, and the image subspace of the controller is composed of the I/O data as the responses to the uncertainties/faults in the plant induced by r_y .*

Recall that r_u delivers the information for cyber-attacks which can be applied for both attack detection and resilient control, while r_y provides the information for process faults for fault detection and fault-tolerant control. The one-to-one mapping between the process data (u, y) and the residual signals (r_u, r_y) , and the role of r_u, r_y in the parameterization of the closed-loop dynamics naturally triggers our inquisitiveness for alternative solutions and modifications on system configuration in the subsequent section.

V. A MODIFIED CPS CONFIGURATION AND THE INTEGRATED DESIGN SCHEME

In this section, a modified CPS configuration is developed. It is followed by the integrated design involving fault detection, attack detection, resilient and fault-tolerant control.

A. A modified CPS configuration

Before proceeding further, the main requirements for the CPS configuration are summarized first: i) achieving ‘‘fail-safe’’ cyber-security, ii) detecting the process faults and cyber-attacks, iii) guaranteeing high fault-tolerance against process faults and high resilience of CPSs under cyber-attacks, iv) ensuring the data privacy, and v) saving online computation and communication effort.

To fulfill the above requirements, we consider the CPS system, which consists of two main parts, the plant with the

embedded sensors and actuators as well as a computing unit, and the monitoring and control (MC) station, at which MC algorithms are implemented. The subsequent CPS configuration (as shown in Fig. 5) is proposed:

- on the plant side, the received signal transmitted by the MC-station is u_{MC}^a ,

$$u_{MC}^a = u_{MC} + a_{u_{MC}}, \quad (28)$$

the performed (online) computation is

$$\begin{cases} \hat{x}(k+1) = (A-LC)\hat{x}(k) + (B-LD)u(k) + Ly(k) \\ r_u(k) = u(k) - F\hat{x}(k) - v_0(k), v_0(z) = Q_v(z)\bar{v}_0(z) \\ r_y(k) = y(k) - \hat{y}(k) = y(k) - C\hat{x}(k) - Du(k) \\ u(z) = F\hat{x}(z) + v_0(z) + u_{MC}^a(z) \\ r_{y,u}(z) = Q_{r,1}(z)r_y(z) + Q_{r,2}(z)r_u(z) \end{cases} \quad (29)$$

where $Q_{r,1}, Q_{r,2} \in \mathcal{RH}_\infty$, Q_v is a pre-filter, \bar{v}_0 is the baseline for the reference, and $r_{y,u}$ is sent to the MC-station,

- at the MC-station, the received signals are

$$r_{y,u}^a = r_{y,u} + a_{r_{y,u}},$$

and the following online computations are performed with u_{MC} being sent to the plant

- for the control purpose

$$\begin{aligned} u_{MC}(z) &= Q_{u_{MC}}(z)(r_{y,u}^a(z) - Q_{r,2}(z)v(z)) + v(z) \\ v(z) &= Q_v(z)(\bar{v}(z) - \bar{v}_0(z)), Q_v \in \mathcal{RH}_\infty \end{aligned} \quad (30)$$

where $Q_{u_{MC}} \in \mathcal{RH}_\infty$ is the design parameter, \bar{v} is the target reference,

- for attack detection

$$\bar{r}_{\eta_a}(z) = \bar{R}(z)(r_{y,u}^a(z) - Q_{r,2}(z)v(z)) \quad (31)$$

where $\bar{R}(z)$ is the post-filter to be designed.

Remark 6. The crucial arguments for the above CPS configuration are

- “fail-safe” cyber-security: With the embedded controller $F\hat{x}(k)$ in (29) at the plant side, the system operation is assured for the case that the communications fail,
- with the embedded v_0 as the baseline of the reference, the transmission of the full information of the target reference v is avoided which increases the data security,
- with $r_{y,u}$ sufficient informations for detection and control are available at the MC-station, and
- the transmission of $r_{y,u}$ instead of the process data y , increases the cyber-security with respect to the data privacy and meanwhile saves the communication effort.

It is noteworthy that a model aware adversary can design attacks by injecting false data which causes damage to the control performance based on the identified process model. To handle this issue, the moving target defense strategies have been widely applied by introducing the time-varying parameters in the control systems [41]. This motivates us to adopt (23) as a time-varying model of the process with $A_{F_{i_k}}, L_{i_k}, F_{i_k}$ belong to a finite set of modes

$$\Gamma = \{(A_{F_1}, L_1, F_1), \dots, (A_{F_\kappa}, L_\kappa, F_\kappa)\}. \quad (32)$$

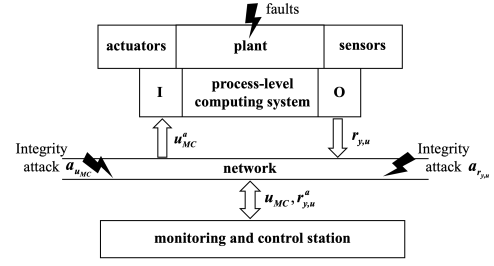


Fig. 3. A modified CPS configuration

Here, i_k represents the index of the process model at the k -th sample. In this sense, $r_{y,u,i}$ with F_{i_k}, L_{i_k} is generated from the plant side, and then $r_{y,u}$ is computed at the MC-station based on the received data $r_{y,u,i}^a = r_{y,u,i} + a_{r_{y,u,i}}$ and Theorem 4. Even though Γ may be available to the attacker, the switching rule will be unknown. As a result, the information available to the defender and the attacker at time k are

$$\begin{aligned} \Gamma_k^d &= \{A, B, C, D, F, L, A_{F_{i_k}}, L_{i_k}, F_{i_k}, u_{MC}^a, y, r_{u,y,i_k}\} \\ \Gamma_k^a &= \{A, B, C, D, F, L, u_{MC}^a, r_{u,y,i_k}\} \end{aligned}$$

respectively. A significant advantage of this moving target scheme over the existing methods lies in adopting the time-varying parameters L_{i_k}, F_{i_k} without changing the process dynamics. To ease the presentation of the design scheme of the CPS system, this issue will not be discussed in details.

Remark 7. Recall that transmitting r_u, r_y to the MC-station makes it easier to cope with detection and control of cyber-attacks and faults. However, it implies increasing data transmissions. Furthermore, transmitting raw data r_u increases the risk of eavesdropping attacks that enable an easy generation of stealthy cyber-attacks. On account of these concerns, the residual $r_{y,u}$ as a fusion of r_y and r_u , as given in (29), is generated and transmitted over the network. In order to reduce the stress of data transmission, the dimension of $r_{y,u}$, and thus the demanded channel capacity, is limited by $\dim(r_{y,u}) = k_y$.

Remark 8. It is noted that one of the major differences of this work with the existing literatures on the attack detection and resilient control of CPSs [26], [42] lies in considering the reference signal v . This is motivated by the engineering practice since v is an essential signal that commends the CPS to perform a defined operation. In particular, such a reference signal is event and task depending and will often be online computed as a part of a decision made on the MC-station.

B. On fault detector design

On account of the fact that the residual signal r_y is perfectly decoupled from cyber-attacks, an observer-based residual generation system running on the plant side is designed for detecting faults. In what follows, the fault detection issue is addressed. To this end, the following Kalman filter is applied

$$\begin{aligned} \hat{x}(k+1) &= A\hat{x}(k) + Bu(k) + L(y(k) - \hat{y}(k)) \\ r_y(k) &= (y(k) - \hat{y}(k)), \hat{y}(k) = C\hat{x}(k) + Du(k) \end{aligned} \quad (33)$$

with

$$\begin{aligned} L &= APC^T \Sigma_{r_y}^{-1}, \Sigma_{r_y} = CPC^T + \Sigma_\nu \\ P &= APA^T + \Sigma_w - APC^T \Sigma_{r_y}^{-1} CPA^T. \end{aligned}$$

As a result, we have $r_y \sim \mathcal{N}(0, \Sigma_{r_y})$. Thus, the following test statistic and threshold with given specification $0 < \alpha < 1$ can be applied for fault detection purpose

$$J_{rel} = r_y^T \Sigma_{r_y}^{-1} r_y \sim \mathcal{X}^2(k_y), J_{rel,th} = \mathcal{X}_\alpha^2(k_y) \quad (34)$$

where $\mathcal{X}^2(k_y)$ denotes the \mathcal{X}^2 distribution with k_y degrees of freedom, and $\mathcal{X}_\alpha^2(k_y)$ is determined based on the chi-squared distribution table.

Remark 9. Recall that the estimates \hat{y} contain full information of the nominal system dynamic, and the generated residuals are of the property $\mathbf{E}(\hat{y}^T r_y) = 0$. In other words, r_y are perpendicular to the estimates and thus do not comprise process information. That means, transmission of residual signals prevents the data privacy efficiently.

C. On attack detector design

Distinguishing from typical technical faults caused by ageing or damage of system components, cyber-attacks are artificially generated signals injected into the system over a certain time interval. It is similar to the so-called intermittent faults [43]. In this regard, the detection task comprises not only detecting injection of cyber-attacks as timely and reliable as possible, but also detecting switching-off of cyber-attacks. In the sequel, these two tasks are addressed separately. The latter is of a special importance for the reason that the cyber-attack resilient control law is to be switched to the nominal controller, once the injected cyber-attacks disappear.

For our purpose, cyber-attack detection is performed at the MC-station under the condition that no fault is detected by the FD system on the plant side. For our purpose, the impact of cyber-attacks on the residual dynamics (31) is examined first.

Theorem 5. Given CPS modelled by (11) with the CPS configuration given in (28)-(30). With the post-filter as

$$\bar{R} = R(I - Q_{r,2}Q_{u_{MC}}), R \in \mathcal{RH}_\infty \quad (35)$$

the residual dynamics (31) is equivalent to

$$\bar{r}_{\eta_a} = R(Q_{r,1}r_y + \eta_a), \eta_a = Q_{r,2}a_{u_{MC}} + a_{r_{y,u}}. \quad (36)$$

Proof. Recall that

$$r_u = Xu + Yy = u - F\hat{x} = u_{MC}^a.$$

As a result, one has that

$$\begin{aligned} r_u &= Q_{u_{MC}}(Q_{r,1}r_y + Q_{r,2}r_u + a_{r_{y,u}} - Q_{r,2}v) + v + a_{u_{MC}} \\ &= (I - Q_{u_{MC}}Q_{r,2})^{-1}(Q_{u_{MC}}Q_{r,1}r_y + \vartheta_a) + v \end{aligned} \quad (37)$$

where $\vartheta_a = Q_{u_{MC}}a_{r_{y,u}} + a_{u_{MC}}$. With the aid of the relation

$$Q_{r,2}(I - Q_{u_{MC}}Q_{r,2})^{-1} = (I - Q_{r,2}Q_{u_{MC}})^{-1}Q_{r,2} \quad (38)$$

one has that

$$Q_{r,2}r_u = (I - Q_{r,2}Q_{u_{MC}})^{-1}Q_{r,2}(Q_{u_{MC}}Q_{r,1}r_y + \vartheta_a) + Q_{r,2}v.$$

Consequently, we have

$$r_{y,u}^a = (I - Q_{r,2}Q_{u_{MC}})^{-1}(Q_{r,1}r_y + \eta_a) + Q_{r,2}v, \quad (39)$$

Algorithm 1 An attack detection algorithm

- 1: Set R as (42) and $\bar{R} = R(I - Q_{r,2}Q_{u_{MC}})$;
- 2: Run the residual generator (31);
- 3: Calculate the test statistic and threshold

$$J = \bar{r}_{\eta_a}^T \bar{r}_{\eta_a} \sim \mathcal{X}^2(k_y), J_{th} = \mathcal{X}_\alpha^2(k_y) \quad (44)$$

- 4: Fault detection by means of the detection logic

$$\text{Detection logic: } \begin{cases} J > J_{th} \implies \text{cyber-attack} \\ J \leq J_{th} \implies \text{attack-free.} \end{cases}$$

which leads to

$$\bar{r}_{\eta_a} = \bar{R}(z)(r_{y,u}^a - Q_{r,2}v) = R(Q_{r,1}r_y + \eta_a) \quad (40)$$

and completes the proof. \square

It is evident that, \bar{r}_{η_a} solely contains redundant information about the plant uncertainties comprised in r_y , when there exists no cyber-attack. Consequently, the detection scheme can be designed depending on the specifications of the plant uncertainties. Assumed that $Q_{r,1}$ has the following state-space representation

$$Q_{r,1} = (A_{r,1}, B_{r,1}, C_{r,1}, D_{r,1}), \quad (41)$$

with $D_{r,1}$ as a full row rank. Recalling that any observer (and so Kalman filter) can be equivalently realized by a post filter, we have the following theorem.

Theorem 6. Consider CPS modelled by (11) with the CPS configuration given in (28)-(30), the residual dynamics (31) with the post-filter as (35). Setting

$$R = (A_{r,1} - LC_{r,1}, -L, \Sigma_{r,1}^{-1/2}C_{r,1}, \Sigma_{r,1}^{-1/2}) \quad (42)$$

with L as the Kalman filter gain satisfying

$$\begin{aligned} L &= (A_{r,1}PC_{r,1}^T + B_{r,1}\Sigma_{r_y}D_{r,1}^T)\Sigma_{r,1}^{-1}, \\ \Sigma_{r,1} &= C_{r,1}PC_{r,1}^T + D_{r,1}\Sigma_{r_y}D_{r,1}^T, \end{aligned} \quad (43)$$

and P as the solution to the following Riccati equation,

$$P - A_{r,1}PA_{r,1}^T - B_{r,1}\Sigma_{r_y}B_{r,1}^T + L\Sigma_{r,1}L^T = 0$$

leads to

$$\begin{aligned} RQ_{r,1} &= (A_{r,1} - LC_{r,1}, B_{r,1} - LD_{r,1}, \Sigma_{r,1}^{-1}C_{r,1}, \Sigma_{r,1}^{-1}D_{r,1}), \\ \bar{r}_{\eta_a} &:= RQ_{r,1}r_y \sim \mathcal{N}(0, I). \end{aligned}$$

From Theorem 6 that the residual \bar{r}_{η_a} contains the necessary information for detecting the cyber-attacks $(a_{u_{MC}}, a_{r_{y,u}})$. Consequently, the χ^2 test statistic

$$\chi^2(k_y) = \bar{r}_{\eta_a}^T \bar{r}_{\eta_a} \underset{\mathcal{H}_1}{\overset{\mathcal{H}_0}{\leq}} J_{th, \chi_\alpha^2}$$

is adopted for the detection end. Thus, Algorithm 1 can be applied for attack detection.

Remark 10. Both $Q_{r,1}, Q_{r,2}$ are, together with $Q_{u_{MC}}$, design parameters for the controller design. In other words, the conditions determined by solving the above-defined detection problem are to be considered, when necessary, as the controller design is addressed. Moreover, although $Q_{r,2}$ is not explicitly included in the model (36), it is a part of the residual generator (29) for $r_{y,u}$, on which the residual r_{η_a} is built.

D. On monitoring of cyber-attacks and detecting switching off of cyber-attacks

We are now in a position to investigate a scheme to monitor and detect the switching off of cyber-attacks. Given the residual model (35)-(36), the main objective is to develop a post-filter R , a test statistic J as well as a threshold so that switching off of cyber-attacks is optimally detected. In our study, it is assumed that residual data $\bar{r}_{\eta_a}(k_0), \dots, \bar{r}_{\eta_a}(k_0 + s)$ are available for the detection purpose, where s is an integer and serves as a hyperparameter.

On account of the resilient control strategy, “weak attacks” can be well tolerated. In this context, it is said

$$\begin{cases} \|\eta_a\|_{RMS,[k,k+\tau]} \leq L_{\eta_a,l} \implies \text{attack-free} \\ \|\eta_a\|_{RMS,[k,k+\tau]} \geq L_{\eta_a,u} \implies \text{cyber-attack.} \end{cases} \quad (45)$$

where $\tau \gg s$, and $L_{\eta_a,l}, L_{\eta_a,u}$ are the lower- and upper-bounds, $L_{\eta_a,l} < L_{\eta_a,u}$.

Now, we begin with the formulation of the detection problem to be addressed. Consider the model

$$\bar{r}_{\eta_a} = RQ_{r,1}r_y + \bar{\eta}_a \sim \mathcal{N}(\bar{\eta}_a, I), \bar{\eta}_a = R\eta_a \in \mathbb{C}^m, \eta_a \in \mathbb{C}^m,$$

and write it into

$$\begin{aligned} \bar{r}_{\eta_a,s}(k_0) &= \varepsilon_{\eta_a,s}(k_0) + \bar{\eta}_{a,s}(k_0), \\ \bar{r}_{\eta_a,s}(k_0) &= \begin{bmatrix} \bar{r}_{\eta_a}(k_0) \\ \vdots \\ \bar{r}_{\eta_a}(k_0 + s) \end{bmatrix}, \bar{\eta}_{a,s}(k_0) = \begin{bmatrix} \bar{\eta}_a(k_0) \\ \vdots \\ \bar{\eta}_a(k_0 + s) \end{bmatrix} \\ \varepsilon_{\eta_a,s}(k_0) &= \begin{bmatrix} \varepsilon_{\eta_a}(k_0) \\ \vdots \\ \varepsilon_{\eta_a}(k_0 + s) \end{bmatrix} \sim \mathcal{N}(0, I). \end{aligned} \quad (46)$$

By means of the state space realisation (42) of R with $x_R(k)$ denoting its state vector, $\bar{\eta}_{a,s}(k_0)$ is written into

$$\begin{aligned} \bar{\eta}_{a,s}(k_0) &= H_{o,s}A_{R,L}^\gamma x_R(k_0 - \gamma) + H_{\bar{\eta}_{a,s},\gamma} \eta_{a,s+\gamma}(k_0 - \gamma + 1) \\ A_{R,L} &= A_{r,1} - LC_{r,1}, B_R = -L, C_R = \Sigma_{r,1}^{-1}C_{r,1}, D_R = \Sigma_{r,1}^{-1}, \end{aligned}$$

$$H_{o,s} = \begin{bmatrix} C_R \\ C_R A_{R,L} \\ \vdots \\ C_R A_{R,L}^s \end{bmatrix}, \eta_{a,s+\gamma}(k_0 - \gamma + 1) = \begin{bmatrix} \eta_a(k_0 - \gamma + 1) \\ \vdots \\ \eta_a(k_0 + s) \end{bmatrix},$$

$$\begin{aligned} H_{\bar{\eta}_{a,s},\gamma} &= [H_{\bar{\eta}_{a,s},\gamma,1} \ H_{\bar{\eta}_{a,s},\gamma,2}], H_{\bar{\eta}_{a,s},\gamma,1} = H_{o,s} [A_{R,L}^{\gamma-1} \ \dots \ A_{R,L}], \\ H_{\bar{\eta}_{a,s},\gamma,2} &= \begin{bmatrix} D_R & 0 & \dots & 0 \\ C_R B_R & D_R & \ddots & \vdots \\ \vdots & \ddots & \ddots & 0 \\ C_R A_{R,L}^{s-1} B_R & \dots & C_R B_R & D_R \end{bmatrix} \in \mathbb{R}^{k_y(s+1) \times k_y(s+1)}. \end{aligned}$$

On the assumption that the integer γ is sufficiently large so that $A_{R,L}^\gamma \approx 0$, $\bar{\eta}_{a,s}(k_0)$ is well approximated by

$$\bar{\eta}_{a,s}(k_0) = H_{\bar{\eta}_{a,s},\gamma} \eta_{a,s+\gamma}(k_0 - \gamma + 1).$$

Note that $\text{rank}(H_{\bar{\eta}_{a,s},\gamma}) \leq k_y(s+1)$. In the sequel, without loss of generality, it is assumed that

$$\text{rank}(H_{\bar{\eta}_{a,s},\gamma}) = k_y(s+1)$$

and $\eta_{a,s+\gamma}(k_0 - \gamma + 1)$ doesn't belong to the null space of $H_{\bar{\eta}_{a,s},\gamma}$, i.e.

$$H_{\bar{\eta}_{a,s},\gamma} \eta_{a,s+\gamma}(k_0 - \gamma + 1) \neq 0.$$

Moreover, the detection logic (45) is re-formulated as

$$\begin{cases} \|\bar{\eta}_{a,s}(k_0)\|^2 \leq \tau \bar{\sigma}_{\min} L_0^2 \implies \text{attack-free} \\ \|\bar{\eta}_{a,s}(k_0)\|^2 > \tau \bar{\sigma}_{\max} L_0^2 \implies \text{cyber-attack} \end{cases} \quad (47)$$

for $\tau = s + \gamma$ and some constant $L_0 > 0$. Here,

$$\bar{\sigma}_{\max} = \lambda_{\max}(H_{\bar{\eta}_{a,s},\gamma} H_{\bar{\eta}_{a,s},\gamma}^T), \bar{\sigma}_{\min} = \lambda_{\min}(H_{\bar{\eta}_{a,s},\gamma} H_{\bar{\eta}_{a,s},\gamma}^T)$$

are the maximum and minimum eigenvalues of $H_{\bar{\eta}_{a,s},\gamma} H_{\bar{\eta}_{a,s},\gamma}^T$, respectively.

The detection logic (47) is interpreted as follows. Suppose that $\eta_{a,s+\gamma}(k_0 - \gamma + 1)$ doesn't belong to the null space of $H_{\bar{\eta}_{a,s},\gamma}$, i.e. $H_{\bar{\eta}_{a,s},\gamma} \eta_{a,s+\gamma}(k_0 - \gamma + 1) \neq 0$. Then,

$$\begin{aligned} \|\bar{\eta}_{a,s}(k_0)\|^2 &= \eta_{a,s+\gamma}^T(k_0 - \gamma + 1) H_{\bar{\eta}_{a,s},\gamma}^T H_{\bar{\eta}_{a,s},\gamma} \eta_{a,s+\gamma}(k_0 - \gamma + 1) \\ \|\bar{\eta}_{a,s}(k_0)\|^2 &\geq \bar{\sigma}_{\min} \eta_{a,s+\gamma}^T(k_0 - \gamma + 1) \eta_{a,s+\gamma}(k_0 - \gamma + 1), \\ \|\bar{\eta}_{a,s}(k_0)\|^2 &\leq \bar{\sigma}_{\max} \eta_{a,s+\gamma}^T(k_0 - \gamma + 1) \eta_{a,s+\gamma}(k_0 - \gamma + 1). \end{aligned}$$

Consequently, together with the detection logic (47), we have

$$\begin{aligned} \|\eta_{a,s+\gamma}(k_0 - \gamma + 1)\|^2 \leq \tau L_0^2 &\iff \sqrt{\frac{1}{\tau} \sum_{i=k_0-\gamma+1}^{k_0+s} \eta_a^T(i) \eta_a(i)} \leq L_0, \\ \|\eta_{a,s+\gamma}(k_0 - \gamma + 1)\|^2 \geq \tau L_0^2 &\iff \sqrt{\frac{1}{\tau} \sum_{i=k_0-\gamma+1}^{k_0+s} \eta_a^T(i) \eta_a(i)} \geq L_0. \end{aligned}$$

Now, given the model (46) and the log-likelihood ratio (LLR)

$$\begin{aligned} \ln \frac{p(\|\bar{\eta}_{a,s}(k_0)\|^2 \leq L_l \mid \bar{r}_{\eta_a,s}(k_0))}{p(\|\bar{\eta}_{a,s}(k_0)\|^2 \geq L_u \mid \bar{r}_{\eta_a,s}(k_0))}, \\ L_l^2 := \tau \bar{\sigma}_{\min} L_0^2, L_u^2 := \tau \bar{\sigma}_{\max} L_0^2, \end{aligned}$$

the detection problem is formulated as finding the LLR

$$J = \ln \frac{\sup_{\bar{\eta}_{a,s}(k_0)} p(\|\bar{\eta}_{a,s}(k_0)\|^2 \leq L_l \mid \bar{r}_{\eta_a,s}(k_0))}{\sup_{\bar{\eta}_{a,s}(k_0)} p(\|\bar{\eta}_{a,s}(k_0)\|^2 \geq L_u \mid \bar{r}_{\eta_a,s}(k_0))} \quad (48)$$

as the test statistic and the corresponding threshold so that $J \stackrel{\mathcal{H}_0}{\leq} J_{th}$, where the null hypothesis \mathcal{H}_0 is for attacks, \mathcal{H}_1 i.e. $\|\eta_a\|_{RMS,[k_0-\gamma+1,k_0-\gamma+\tau]} \geq L_0$, and the alternative hypothesis is for attack-free, $\|\eta_a\|_{RMS,[k+1,k+\tau]} < L_0$. Below, the solution is outlined.

Theorem 7. Considering the model (46), the solution to (48) is given by

$$J = \begin{cases} \frac{1}{2} \left(\|\bar{r}_{\eta_a,s}(k_0)\| - L_u \right)^2, \|\bar{\eta}_{a,s}(k_0)\|^2 \leq L_l^2 \\ \frac{1}{2} \left(\|\bar{r}_{\eta_a,s}(k_0)\| - L_l \right)^2, L_l^2 \leq \|\bar{\eta}_{a,s}(k_0)\|^2 \leq L_u^2 \\ -\frac{1}{2} \left(\|\bar{r}_{\eta_a,s}(k_0)\| - L_l \right)^2, \|\bar{\eta}_{a,s}(k_0)\|^2 \geq L_u^2. \end{cases}$$

Proof. To begin with, J in (48) is written into

$$J = \frac{1}{2} \sup_{\substack{\bar{\eta}_{a,s}(k_0) \\ \|\bar{\eta}_{a,s}(k_0)\|^2 \leq L_l^2}} - \|\bar{r}_{\eta_{a,s}}(k_0) - \bar{\eta}_{a,s}(k_0)\|^2 \\ - \frac{1}{2} \sup_{\substack{\bar{\eta}_{a,s}(k_0) \\ \|\bar{\eta}_{a,s}(k_0)\|^2 \geq L_u^2}} - \|\bar{r}_{\eta_{a,s}}(k_0) - \bar{\eta}_{a,s}(k_0)\|^2,$$

which can be solved equivalently by means of the following two optimisation problems,

$$\frac{1}{2} \inf_{\substack{\bar{\eta}_{a,s}(k_0) \\ \|\bar{\eta}_{a,s}(k_0)\|^2 \leq L_l^2}} \|\bar{r}_{\eta_{a,s}}(k_0) - \bar{\eta}_{a,s}(k_0)\|^2, \\ \frac{1}{2} \inf_{\substack{\bar{\eta}_{a,s}(k_0) \\ \|\bar{\eta}_{a,s}(k_0)\|^2 \geq L_u^2}} \|\bar{r}_{\eta_{a,s}}(k_0) - \bar{\eta}_{a,s}(k_0)\|^2.$$

Accordingly, it turns out, for $\|\bar{\eta}_{a,s}(k_0)\|^2 \leq L_l^2$,

$$J = \frac{1}{2} \|\bar{r}_{\eta_{a,s}}(k_0) - \hat{\eta}_{a,s}^u(k_0)\|^2, \hat{\eta}_{a,s}^u(k_0) = \frac{\bar{r}_{\eta_{a,s}}(k_0) L_u}{\sqrt{\bar{r}_{\eta_{a,s}}^T(k_0) \bar{r}_{\eta_{a,s}}(k_0)}},$$

for $\|\bar{\eta}_{a,s}(k_0)\|^2 \geq L_u^2$,

$$J = \frac{1}{2} \|\bar{r}_{\eta_{a,s}}(k_0) - \hat{\eta}_{a,s}^l(k_0)\|^2, \hat{\eta}_{a,s}^l(k_0) = \frac{\bar{r}_{\eta_{a,s}}(k_0) L_l}{\sqrt{\bar{r}_{\eta_{a,s}}^T(k_0) \bar{r}_{\eta_{a,s}}(k_0)}},$$

and for $L_l^2 \leq \|\bar{\eta}_{a,s}(k_0)\|^2 \leq L_u^2$,

$$J = \frac{1}{2} \|\bar{r}_{\eta_{a,s}}(k_0) - \hat{\eta}_{a,s}^u(k_0)\|^2 - \frac{1}{2} \|\bar{r}_{\eta_{a,s}}(k_0) - \hat{\eta}_{a,s}^l(k_0)\|^2.$$

After some routine calculations, the proof is completed. \square

Next, a threshold J_{th} is determined under the condition of a (maximum) false alarm rate (FAR) equal to α . That means

$$\sup_{\substack{\bar{\eta}_{a,s}(k_0) \\ \|\bar{\eta}_{a,s}(k_0)\|^2 \geq L_u^2}} \Pr(J > J_{th} | \bar{r}_{\eta_{a,s}}(k_0) \sim \mathcal{N}(\bar{\eta}_{a,s}(k_0), I)) = \alpha.$$

Observe that the core of the LLR J is $(\|\bar{r}_{\eta_{a,s}}(k_0)\| - L_\mu)^2$, $\mu = l, u$. Let

$$(\|\bar{r}_{\eta_{a,s}}(k_0)\| - L_\mu)^2 = J_\mu(\bar{r}_{\eta_{a,s}}(k_0)).$$

Then,

$$(J_\mu^{1/2}(\bar{r}_{\eta_{a,s}}(k_0)) + L_\mu)^2 = \|\bar{r}_{\eta_{a,s}}(k_0)\|^2.$$

Recall that $\|\bar{r}_{\eta_{a,s}}(k_0)\|^2$ is subject to a non-central χ^2 distribution with $(s+1)m$ degrees of freedom and the non-centrality parameter $\|\bar{\eta}_{a,s}(k_0)\|^2$. Since $\bar{\eta}_{a,s}(k_0)$ is unknown and no a prior information of $\bar{\eta}_{a,s}(k_0)$ is available, it is suggested to calculate the FAR with respect to $\|\bar{\eta}_{a,s}(k_0)\|^2 = L_u^2$. This means, we check the FAR corresponding to the lower-bound of the $\|\bar{\eta}_{a,s}(k_0)\|^2$, when attacks exist. In a certain sense, this is the worst case. As a result, we finally have

$$(J_\mu^{1/2}(\bar{r}_{\eta_{a,s}}(k_0)) + L_\mu)^2 = \|\bar{r}_{\eta_{a,s}}(k_0)\|^2 \sim \chi^2((s+1)m, L_u^2),$$

and based on it, the threshold J_{th} can be calculated.

E. On the resilient and fault-tolerant control

To this end, we first re-examined the process dynamics for the CPS configuration (28)-(30).

Corollary 3. *Given CPS modelled by (11) with the CPS configuration given in (28)-(30), then the closed-dynamics is governed by*

$$\begin{bmatrix} u \\ y \end{bmatrix} = \begin{bmatrix} M \\ N \end{bmatrix} \left(v + (I - Q_{u_{MC}} Q_{r,2})^{-1} \vartheta_a \right) + \begin{bmatrix} -\hat{Y} \\ \hat{X} \end{bmatrix} + \begin{bmatrix} M \\ N \end{bmatrix} Q_{u_{MC}} \bar{Q}_{r,1} r_y \\ \vartheta_a := Q_{u_{MC}} a_{r_y, u} + a_{u_{MC}}, \bar{Q}_{r,1} = (I - Q_{r,2} Q_{u_{MC}})^{-1} Q_{r,1} \quad (49)$$

Proof. It follows from the proof of Theorem 5 that

$$u_{MC}^a = v + (I - Q_{u_{MC}} Q_{r,2})^{-1} (Q_{u_{MC}} Q_{r,1} r_y + \vartheta_a). \quad (50)$$

Since

$$\begin{bmatrix} u \\ y \end{bmatrix} = \begin{bmatrix} X & Y \\ -\hat{N} & \hat{M} \end{bmatrix}^{-1} \begin{bmatrix} u_{MC}^a \\ r_y \end{bmatrix} \quad (51)$$

the closed-loop dynamic is described by (49). \square

Recall that the faults and the corresponding control performance degradations in the plant solely cause variations in the system residual subspace and the attacks only lead to changes in the system image subspace. Based on it, we are now in the position to propose a resilient and FTC scheme. Given $1 > \gamma_{r_y} > 0$ and $1 > \gamma_{\vartheta_a} > 0$ that represent the resilient and FTC performance, find $Q_{r,1}, Q_{r,2}$ and $Q_{u_{MC}}$ such that $(I - Q_{u_{MC}} Q_{r,2})^{-1}$ is stable, and

$$\|(I - Q_{u_{MC}} Q_{r,2})^{-1}\|_\infty \leq \gamma_{\vartheta_a}, \quad (52)$$

$$\left\| \begin{bmatrix} -\hat{Y} \\ \hat{X} \end{bmatrix} + \begin{bmatrix} M \\ N \end{bmatrix} Q_{u_{MC}} \bar{Q}_{r,1} \right\|_\infty \leq \gamma_{r_y}. \quad (53)$$

Remark 11. *It is plait that the condition (53) describes the system robustness against the potential faults presented by the residual r_y , while the condition (52) imposes the resilient requirement dealing with the cyber-attack ϑ_a . Observe that for the resilient controller subject to (52)-(53), $Q_{r,1}, Q_{r,2}$ and $Q_{u_{MC}}$ are redundant. In fact, $Q_{r,2}$ can be used as an encoder to complicate the construction of a stealthy attack vector η_a defined in (36). In this case, $Q_{u_{MC}}$ is firstly determined given $Q_{r,2}$, and then $Q_{r,1}$ is found for given $Q_{u_{MC}}$.*

VI. STEALTHY ATTACKS AND PERFORMANCE-BASED DETECTION

Stealthy attacks are such attacks that will not cause detectable changes in the detection test statistic aiming at degrading the system control performance. From the defender's point of view, it is of importance to study the potential stealthy attacks, and more importantly, develop the corresponding detection schemes. To this end, the stealthy attack design against tracking behaviour and feedback control performance are studied in this section. It is followed by the associated detection schemes.

A. Stealthy attack design against tracking behaviour

The definition of stealthy attacks is given first.

Definition 3. An attack is said to be stealthy if the residual signals satisfy

$$r_{y,u}^a \sim \mathcal{N}\left(\mathbb{E}r_{y,u}^a, \Sigma_{r_{y,u}^a}\right), \Sigma_{r_{y,u}^a} = \Sigma_{r_{y,u}}, \mathbb{E}r_{y,u}^a = \mathbb{E}r_{y,u} \quad (54)$$

It follows from the closed-loop dynamic (49), that the cyber-attack ϑ_a degrades the system tracking behaviour, while a change of the feedback mechanism of r_y will lead to feedback performance degradation. Examining the dynamics of the residual generator (36) leads to the following lemma.

Lemma 2. Consider the CPS configuration (28)-(30). The following attack is stealthy

$$\eta_a = Q_{r,2}a_{u_{MC}} + a_{r,y,u} = 0. \quad (55)$$

It is apparent that, to attack the system tracking behaviour stealthily, the attack design is to be formulated as maximising the tracking error,

$$\begin{bmatrix} \Delta u \\ \Delta y \end{bmatrix} := \begin{bmatrix} u \\ y \end{bmatrix} - \begin{bmatrix} M \\ N \end{bmatrix} v = \begin{bmatrix} M \\ N \end{bmatrix} (I - Q_{u_{MC}}Q_{r,2})^{-1} \vartheta_a,$$

by selecting $\vartheta_a = Q_{u_{MC}}a_{r,y,u} + a_{u_{MC}}$ subject to (55). From the condition (55), the following relations automatically arise,

$$\vartheta_a = (I - Q_{u_{MC}}Q_{r,2})a_{u_{MC}} \implies \begin{bmatrix} \Delta u \\ \Delta y \end{bmatrix} = \begin{bmatrix} M \\ N \end{bmatrix} a_{u_{MC}} \quad (56)$$

which indicates that the tracking performance degradation solely depends on $a_{u_{MC}}$.

Remark 12. It is interesting to notice that the condition (55) is similar to the so-called covert attacks [44]. The difference between them lies in the transfer function $Q_{r,2}$, which is the transfer function of the plant in case of a covert attack. Specifically, $Q_{r,2}$ in (55) is a design parameter and can also be online updated during system operations, while the transfer function of the plant is fixed. This fact makes the realization of such stealthy attacks more difficult.

B. Stealthy attack design against feedback control performance

Remember that cyber-attacks cause no change in the residual r_y . This implies that degrading the system feedback dynamics can only be achieved by changing the following feedback mechanism

$$\begin{bmatrix} -\hat{Y} \\ \hat{X} \end{bmatrix} + \begin{bmatrix} M \\ N \end{bmatrix} Q_{u_{MC}} \bar{Q}_{r,1}. \quad (57)$$

Thus, the stealthy attack design issue against feedback control performance can be formulated as follows:

Given $r_{y,u} \sim \mathcal{N}(0, \Sigma_{r_{y,u}})$, $r_{y,u} \in \mathcal{R}^{k_y}$ denoting the nominal (attack-free) residual, find a linear mapping of $r_{y,u}$

$$r_{y,u}^a = f(r_{y,u}) \in \mathcal{R}^{k_y} \quad (58)$$

such that (54) holds and the feedback performance (57) is deteriorated as much as possible, that is, $Q_{u_{MC}}\bar{Q}_{r,1}$ is modified so that the norm of (57) becomes larger.

For our purpose, the following attack model is considered

$$r_{y,u}^a = \Pi_a (r_{y,u} - \zeta) + \zeta \quad (59)$$

where Π_a is the attack matrix to be designed. Below, a realistic and practical scenario for constructing stealthy cyber-attacks is developed that degrade the feedback control performance.

Assumption 1. It is assumed that the CPS system under consideration is operating in the steady state with a constant reference vector in the attack-free case so that the residual vector $r_{y,u}$ is a weakly stationary stochastic process as

$$\mathbb{E}r_{y,u} = \lim_{z \rightarrow 1} Q_{r,2}v =: \zeta, \Sigma_{r_{y,u}} = \mathbb{E}(r_{y,u} - \zeta)(r_{y,u} - \zeta)^T, \\ r_{y,u} - \zeta = (I - Q_{r,2}Q_{u_{MC}})^{-1} Q_{r,1}r_y,$$

where ζ and $\Sigma_{r_{y,u}}$ are constant vector and matrix, respectively.

Suppose that attackers collect (sufficient) N number of data of $r_{y,u}$ over the time interval $[k_1, k_N]$ and calculate the maximal likelihood estimates of ζ and $\Sigma_{r_{y,u}}$,

$$\hat{\zeta} = \frac{1}{N} \sum_{i=1}^N \zeta(k_i), \hat{\Sigma}_{r_{y,u}} = \frac{1}{N} \sum_{i=1}^N (r_{y,u}(k_i) - \hat{\zeta})(r_{y,u}(k_i) - \hat{\zeta})^T.$$

Theorem 8. Consider the CPS configuration (28)-(30), the stealthy attacks can be constructed as follows:

$$r_{y,u}^a = \Pi_a (r_{y,u} - \hat{\zeta}) + \hat{\zeta}, \Pi_a = \Xi \Pi \quad (60)$$

where Π is a Kalman filter satisfying

$$\hat{x}_\Pi(k+1|k) = A_\Pi \hat{x}_\Pi(k|k-1) + K(k)\Delta r_{y,u}(k), \\ \Delta r_{y,u}(k) = r_{y,u}(k) - \hat{\zeta} - C_\Pi \hat{x}_\Pi(k|k-1), \hat{x}_\Pi(0) = 0, \\ K(k) = A_\Pi P(k|k-1)C_\Pi^T \Sigma_{\Delta r_{y,u}}^{-1}(k), \\ P(k+1|k) = A_\Pi P(k|k-1)A_\Pi^T - K(k)\Sigma_{\Delta r_{y,u}}(k)K^T(k), \\ \Sigma_{\Delta r_{y,u}}(k) = C_\Pi P(k|k-1)C_\Pi^T + \hat{\Sigma}_{r_{y,u}},$$

and Ξ is a matrix

$$\Xi = U \hat{\Sigma}_{r_{y,u}}^{1/2} \Sigma_{\Delta r_{y,u}}^{-1/2}, U U^T = I.$$

Proof. It is easy to examine that

$$\mathbb{E}r_{y,u}^a = \mathbb{E}r_{y,u} = \zeta, \Sigma_{r_{y,u}^a} = \mathbb{E}(r_{y,u}^a - \zeta)(r_{y,u}^a - \zeta)^T = \Sigma_{r_{y,u}}$$

so that the added cyber-attack is (strictly) stealthy. \square

Remark 13. Notice that the attack (60) is stealthy independent of the test statistic implemented on the attack detection, and hence holds also for Kullback-Leibler divergence (KLD) based test statistic [14], [45].

Moreover, the feedback control performance is governed by

$$\begin{bmatrix} u_f \\ y_f \end{bmatrix} = \left(\begin{bmatrix} -\hat{Y} \\ \hat{X} \end{bmatrix} + \begin{bmatrix} M \\ N \end{bmatrix} Q_{u_{MC}} \Pi_a \bar{Q}_{r,1}^a \right) r_y \quad (61)$$

$$\bar{Q}_{r,1}^a = (I - Q_{r,2}Q_{u_{MC}}\Pi_a)^{-1} Q_{r,1}$$

which implies that the cyber-attack (60) can degrade the system feedback control performance. Consequently, setting $\Pi_a = \Xi \Pi = -I$ could considerably degrade the feedback performance. In other words, without any process model knowledge, constructing the stealthy cyber-attack simply as

$$r_{y,u}^a = -(r_{y,u} - \zeta) + \zeta = -r_{y,u} + 2\zeta \implies \\ \begin{bmatrix} u_f \\ y_f \end{bmatrix} = \left(\begin{bmatrix} -\hat{Y} \\ \hat{X} \end{bmatrix} - \begin{bmatrix} M \\ N \end{bmatrix} Q_{u_{MC}} (I + Q_{r,2}Q_{u_{MC}})^{-1} Q_{r,1} \right) r_y$$

can result in a remarkable degradation of the system robustness.

Remark 14. *The cyber-attacks $\Pi_a r_y$ has been well studied with Π_a as a unitary matrix in [26], [45]–[48]. It is noteworthy that availability of process model knowledge or collection of sufficient amount of data, by which process model can be identified, are the widely accepted and adopted assumptions, on which the developed design methods for stealthy attacks are based. On the other hand, attacks on the estimation performance of the embedded observer are the focus of the existing research, both for control and (remote) monitoring of CPSs [6], [24], while limit attention has been made on attack against feedback control performance.*

C. Performance degradation monitoring-based detection of stealthy attacks against feedback performance

In the subsequent subsections, we are devoted to develop detection schemes for monitoring the performance degradation caused by the stealthy attacks against feedback performance and tracking behavior, respectively.

Without loss of generality, the stealthy attacks on the system feedback result in the change on feedback dynamics as (61). That means, the signal r_{PD} generated by

$$r_{PD} = \Psi \left(\begin{bmatrix} -\hat{Y} \\ \hat{X} \end{bmatrix} + \begin{bmatrix} M \\ N \end{bmatrix} Q_{u_{MC}} \Pi_a \bar{Q}_{r,1}^a \right) r_y \quad (62)$$

is the information carrier of degradation in feedback control performance that is capable for detecting performance degradation caused by cyber-attacks. Here, $\Psi \in \mathcal{RH}_\infty$ is an arbitrary stable dynamic system.

Motivated by the aforementioned discussion and the residual (62), we now propose to construct $r_{y,u}$ as follows,

$$r_{y,u} = Q_{r,1} r_y + Q_{r,2} r_u + \bar{r}_{PD}, \bar{r}_{PD} = \Psi \begin{bmatrix} u \\ y \end{bmatrix} \quad (63)$$

Corresponding to the nominal control law (29), the controller is now set as

$$\begin{aligned} u &= F \hat{x} + u_{MC} - Q_{u_{MC}} \bar{r}_{PD}, \\ u_{MC} &= Q_{u_{MC}} (r_{y,u}^a - Q_{r,2} v) + v. \end{aligned} \quad (64)$$

Let

$$r_{y,u}^a = \Pi_a (r_{y,u} - Q_v v) + Q_v v, Q_v := \Psi \begin{bmatrix} M \\ N \end{bmatrix} v \quad (65)$$

with Π_a as the cyber-attack system, and assume that attackers are in possession of knowledge of $Q_v v$ or $Q_v v$ is sufficiently small so that it can be neglected.

The subsequent work is dedicated to the analysis of residual dynamics under such cyber-attacks and, based on it, the development of a performance degradation detection scheme. It follows from (63)-(65) that

$$\begin{aligned} \begin{bmatrix} u \\ y \end{bmatrix} &= \begin{bmatrix} M \\ N \end{bmatrix} (I + Q_{u_{MC}} \bar{\Pi}_a) v + \left(\begin{bmatrix} -\hat{Y} \\ \hat{X} \end{bmatrix} + \begin{bmatrix} M \\ N \end{bmatrix} Q_{u_{MC}} \Pi_a \bar{Q}_{r,1}^a \right) r_y \\ &\quad + \begin{bmatrix} M \\ N \end{bmatrix} Q_{u_{MC}} \Pi_a \bar{Q}_{r,2}^a Q_{u_{MC}} (\Pi_a - I) \Psi \left(\begin{bmatrix} u \\ y \end{bmatrix} - \begin{bmatrix} M \\ N \end{bmatrix} v \right) \end{aligned}$$

After some routine calculations, we have

$$\begin{bmatrix} u \\ y \end{bmatrix} = \begin{bmatrix} M \\ N \end{bmatrix} (I + Q_{u_{MC}} \Phi_1 \bar{\Pi}_a) v + \left(\begin{bmatrix} -\hat{Y} \\ \hat{X} \end{bmatrix} + \begin{bmatrix} M \\ N \end{bmatrix} \Phi_1 \Phi_2 \right) r_y, \quad (66)$$

where

$$\begin{aligned} \Phi_1 &= Q_{u_{MC}} \left(I - (\Pi_a \bar{Q}_{r,2}^a Q_{u_{MC}} (\Pi_a - I) - I) \Psi \begin{bmatrix} M \\ N \end{bmatrix} Q_{u_{MC}} \right)^{-1} \\ \Phi_2 &= \Pi_a \bar{Q}_{r,1}^a + (\Pi_a \bar{Q}_{r,2}^a Q_{u_{MC}} (\Pi_a - I) - I) \Psi \begin{bmatrix} -\hat{Y} \\ \hat{X} \end{bmatrix} \\ \bar{\Pi}_a &= \Pi_a \bar{Q}_{r,2}^a (I - Q_{u_{MC}} Q_{r,2}) - Q_{r,2} - \Pi_a Q_v + Q_v \\ \bar{Q}_{r,1}^a &= (I - Q_{r,2} Q_{u_{MC}} \Pi_a)^{-1} Q_{r,1}, \bar{Q}_{r,2}^a = (I - Q_{u_{MC}} \Pi_a)^{-1} Q_{r,2} \end{aligned}$$

It can be seen clearly that during attack-free operations, i.e. $\Pi_a = I$, (66) is exactly the nominal closed-loop dynamic, and the feedback performance degradation caused by $\Pi_a \neq I$ is modelled by

$$\begin{bmatrix} u_f \\ y_f \end{bmatrix} = \left(\begin{bmatrix} -\hat{Y} \\ \hat{X} \end{bmatrix} + \begin{bmatrix} M \\ N \end{bmatrix} \Phi_1 \Phi_2 \right) r_y.$$

Consequently, it holds

$$r_{y,u}^a = (\bar{\Pi}_a + Q_{r,2} + \Phi_3) v + \Pi_a \left(\bar{Q}_{r,1}^a + \Gamma \Psi \left(\begin{bmatrix} -\hat{Y} \\ \hat{X} \end{bmatrix} + \begin{bmatrix} M \\ N \end{bmatrix} \Phi_1 \Phi_2 \right) \right) r_y$$

$$\Gamma = \bar{Q}_{r,2}^a Q_{u_{MC}} (\Pi_a - I)$$

$$\Phi_3 = \Pi_a \bar{Q}_{r,2}^a Q_{u_{MC}} \left((\Pi_a - I) Q_v - \begin{bmatrix} M \\ N \end{bmatrix} Q_{u_{MC}} \Phi_1 \bar{\Pi}_a \right) + Q_v$$

Hence, residual signal

$$r_{PDD}^a := r_{y,u}^a - (Q_{r,2} + Q_v) v \quad (67)$$

contains the full information about the feedback performance degradation and can be used for the detection purpose. To this end, design Ψ so that

$$\gamma_\Psi := \left\| \Psi \left(\begin{bmatrix} -\hat{Y} \\ \hat{X} \end{bmatrix} + \begin{bmatrix} M \\ N \end{bmatrix} \Phi_1 \Phi_2 \right) \right\|_2 \gg \|\bar{Q}_{r,1}\|_2, \quad (68)$$

where $\|\cdot\|_2$ denotes \mathcal{H}_2 -norm of a transfer function. On account of the fact that the cyber-attacks target at reducing the system robustness leading to a larger γ_Ψ , it is expected that (68) holds.

Considering that Π_a should be an inner, the condition of attack stealthiness, the standard generalized likelihood ratio (GLR) detection schemes can be applied to detect the attacks. To be specific, during attack-free operation, the covariance matrix of r_{PDD} can be calculated based on the model

$$r_{PDD} = \left(\bar{Q}_{r,1} + \Psi \left(\begin{bmatrix} -\hat{Y} \\ \hat{X} \end{bmatrix} + \begin{bmatrix} M \\ N \end{bmatrix} Q_{u_{MC}} \bar{Q}_{r,1} \right) \right) r_y.$$

To simplify the online implementation of the detection algorithm, a post-filter $R(z)$ can be added so that

$$\bar{r}_{PDD}(z) = R(z) r_{PDD}(z) \sim \mathcal{N}(0, \Sigma_{\bar{r}_{PDD}}).$$

Supposed that N data, $\bar{r}_{PDD}^a(k+i)$, $i = 1, \dots, N$, have been collected. Using the GLR detection method, we have the test statistic

$$\begin{aligned} J &= \frac{N}{2} \ln \frac{\det(\Sigma_{\bar{r}_{PDD}})}{\det(\hat{\Sigma}_{\bar{r}_{PDD}^a})} \\ &\quad + \frac{1}{2} \sum_{i=1}^N \left(\bar{r}_{PDD}^a(k+i) \right)^T \left(\Sigma_{\bar{r}_{PDD}}^{-1} - \hat{\Sigma}_{\bar{r}_{PDD}^a}^{-1} \right) \bar{r}_{PDD}^a(k+i), \\ \hat{\Sigma}_{\bar{r}_{PDD}^a} &= \frac{1}{N} \sum_{i=1}^N \bar{r}_{PDD}^a(k+i) \left(\bar{r}_{PDD}^a(k+i) \right)^T, \end{aligned}$$

and determine the threshold accordingly.

D. Detection of stealthy attacks against tracking performance

We next address the detection issue for the (additive) stealthy attacks subject to (55). To this end, the residual (63) is constructed and the controller is set to be

$$\begin{aligned} u &= F\hat{x} + u_{MC}^a - Q_{u_{MC}}\bar{r}_{PD}, \\ u_{MC} &= Q_{u_{MC}}(r_{y,u}^a - Q_{r,2}v) + v. \end{aligned}$$

Next, we examine the system dynamics. It can be easily seen that for the stealthy attacks $Q_{r,2}a_{u_{MC}} + a_{r_{y,u}} = 0$, we have

$$u = F\hat{x} + v + a_{u_{MC}} + (I - Q_{u_{MC}}Q_{r,2})^{-1}Q_{u_{MC}}Q_{r,1}r_y,$$

which results in

$$\begin{aligned} r_{y,u}^a &= \Gamma r_y + Q_{r,2}v + \Psi \left(\begin{bmatrix} M \\ N \end{bmatrix} (v + a_{u_{MC}}) \right) \\ \Gamma &= \Psi \left(\begin{bmatrix} -\hat{Y} \\ \hat{X} \end{bmatrix} + \begin{bmatrix} M \\ N \end{bmatrix} Q_{u_{MC}}\bar{Q}_{r,1} \right) + \bar{Q}_{r,1}. \end{aligned}$$

Thus, builds the following residual signal

$$r_{PDD}^a := r_{y,u}^a - (Q_{r,2} + Q_v)v = Q_v a_{u_{MC}} + \Gamma r_y. \quad (69)$$

Since $r_y \sim \mathcal{N}(0, \Sigma_{r_y})$, χ_2 test statistic can be applied for detecting $a_{u_{MC}}$ on the basis of model (69).

Remark 15. In the paper, three different forms of the residual signal have been proposed, (29), (67) and (69). While the first one is applied to the detection of cyber-attacks in general, the latter two are dedicated to detecting stealthy attacks. It is noteworthy that, independent of which of the three residual forms is adopted, the overall closed-loop dynamics under attack-free operations are identical with the nominal system dynamic. For a reliable detection of cyber-attacks with high resilience, a schedule mechanism is to be designed that manages switchings among the three detection algorithms. For instance, run the detection algorithm based the residual $r_{y,u}$ (29) as the base detection scheme, and switch to an algorithm with residual (67) or (69) over a short time interval, and then return to the base detection scheme. A meaningful side-effect of such a schedule mechanism is to enhance the resilience against eavesdropping attacks, which is a typical strategy followed by a cyber adversary to design stealthy attacks.

VII. AN EXPERIMENTAL STUDY

In this section, a leader-follower robot system, as illustrated in Fig. 4, is adopted to demonstrate our proposed methods.

A. System configuration

In this study, the leader generates the reference velocities, which are then tracked by the follower. In this context, the leader serves as the MC station for the follower. Specifically, the follower sends the residual $r_{y,u}$ to the leader and receives the control input u_{MC} from it, which contains the reference velocities. Their inputs and outputs are the setpoint speeds for three motors and three velocities, namely horizontal, vertical,

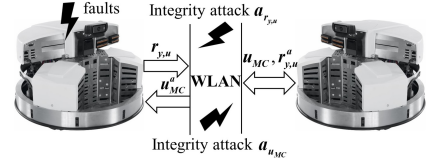


Fig. 4. The system configuration

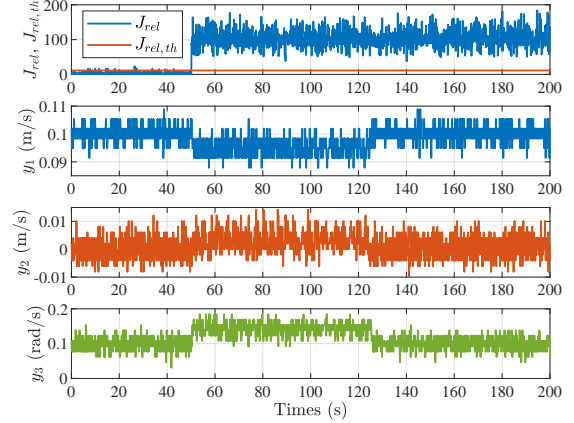


Fig. 5. Fault detection and fault-tolerant control

and angular velocity. With the sampling rate of 10 Hz, the state-space model for the follower is

$$A_f = \begin{bmatrix} 0.428 & 0.020 & 0.0001 \\ 0.026 & 0.419 & 0.0037 \\ 0.284 & -0.09 & 0.2922 \end{bmatrix}, B_f = \begin{bmatrix} -0.685 & 0.025 & 0.655 \\ 0.406 & -0.803 & 0.344 \\ 4.012 & 3.494 & 3.346 \end{bmatrix} \times 10^{-4}$$

with $C_f = \text{diag}\{1, 1, 1\}$, $D_f = 0$ and zero initial conditions. The noise covariance matrices are estimated based on the measurements. On the plant side, one observer, observer-based residual generator, and controller are constructed according to (29). The state feedback gain F is initialized as the LQ gain, and the observer gain L is set as the Kalman gain given in (33). The parameters $Q_{r,1}$, $Q_{r,2}$, and $Q_{u_{MC}}$ are initialized as

$$\begin{aligned} Q_{r,1} &= \text{diag}\{(z-0.1)^{-1}, (z-0.1)^{-1}, (z-0.1)^{-1}\} \\ Q_{r,2} &= -0.15(z+0.1)^{-1} \text{diag}\{(z+0.4), (z+0.3), (z+0.2)\} \\ Q_{u_{MC}} &= \text{diag}\left\{ \frac{10(z+0.1)}{z+0.4}, \frac{10(z+0.1)}{z+0.3}, \frac{10(z+0.1)}{z+0.2} \right\}. \quad (70) \end{aligned}$$

The achieved performance levels are $\gamma_{\vartheta_a} = 0.4000$, $\gamma_{r_y} = 6.2406$. The feedforward controller T is selected as

$$T = \begin{bmatrix} -4257.4943 & 2463.2315 & 662.2074 \\ 10.9463 & -4940.2157 & 664.6608 \\ 4284.4037 & 2462.1782 & 663.4313 \end{bmatrix}. \quad (71)$$

B. Fault detection and fault-tolerant control

For our purpose, the bias fault $f \sim \mathcal{N}(0.025, 1 \times 10^{-6})$ of the first sensor is injected from the time instant [50s, 125s]. Setting the FAR as 0.01 leads to $J_{rel,th} = 11.3450$. As shown in the first subfigure of Fig. 5, the fault can be well detected.

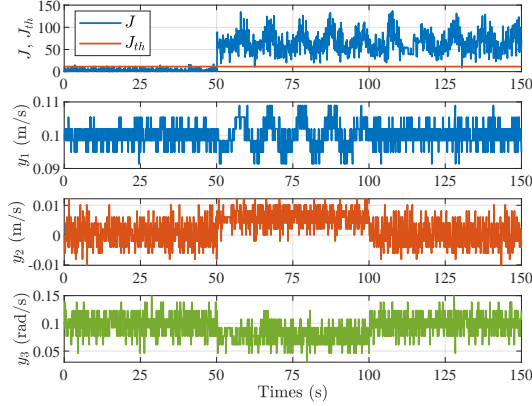


Fig. 6. Detection and resilient control of the cyber-attack

For FTC purpose, $Q_{r,2}$ is reconfigured as

$$Q_{r,2} = -90(z+0.1)^{-1} \text{diag} \{ (z+0.4), (z+0.3), (z+0.2) \}$$

with $Q_{u_{MC}}$ given by (70). The associated performance level is $\gamma_{\vartheta_a} = 1.1099 \times 10^{-3}$. Based on the obtained $Q_{r,2}$ and $Q_{u_{MC}}$, $Q_{r,1}$ is attained by solving (55) via the *hinfsyn* command in MATLAB. The achieved performance level is $\gamma_{r_y} = 1.0997$. For demonstration purpose, the controller is reconfigured in the time interval of [125 s, 200 s]. According to the output velocity trajectories y_1, y_2, y_3 of Fig. 5, the sensor fault can be well compensated by reconfiguring the fault-tolerant controller.

C. Attack detection and attack-resilient control

In this study, the following attacks are injected into the corresponding channels during the time interval [50 s, 150 s]

$$a_{u_{MC}}(k) = [a_{u_{MC,1}}(k) \ 0 \ a_{u_{MC,3}}(k)]^T \quad (72)$$

$$a_{u_{MC,1}}(k) = 0.05 \sin(0.2\pi k), \ a_{u_{MC,3}}(k) = -0.05 \sin(0.2\pi k)$$

$$a_{r_{y,u}}(k) = [0 \ a_{r_{y,u,2}}(k) \ 0]^T, \ a_{r_{y,u,2}} \sim \mathcal{N}(-0.025, 1 \times 10^{-10}).$$

Based on (42), the post-filter R for attack detection purpose is given. Setting the FAR as 0.01 leads to $J_{th} = 11.3450$. As shown in the first subfigure of Fig. 6, these additive attacks can be well detected. Then, the controller is reconfigured during the time interval of [100 s, 150 s]. As described in Fig. 6, the attack-induced variations in robot velocities can be largely reduced, which verifies the effectiveness of the resilient controller.

D. Detection of attack switching-on and switching-off

For our purpose, the parameters s , γ , and L_0 are selected as $s = 30$, $\gamma = 500$, $L_0 = 1 \times 10^{-4}$, $\tau = 530$. Then, the lower and upper bound L_l and L_u are calculated as $L_l = 0.1433$, $L_u = 1.0474$. According to the non-central χ^2 distribution table, setting $\|\bar{r}_{\eta_a,s}(k_0)\|_2^2 = 129.15$ gives the FAR as 0.01. Consequently, the thresholds for the evaluation functions in (50) are given by

$$J_{th} = \begin{cases} 53.2207, & \|\bar{r}_{\eta_a,s}(k_0)\|_2^2 \leq L_l^2, \\ -9.7366, & L_l^2 \leq \|\bar{r}_{\eta_a,s}(k_0)\|_2^2 \leq L_u^2, \\ -62.9573, & \|\bar{r}_{\eta_a,s}(k_0)\|_2^2 \geq L_u^2. \end{cases} \quad (73)$$

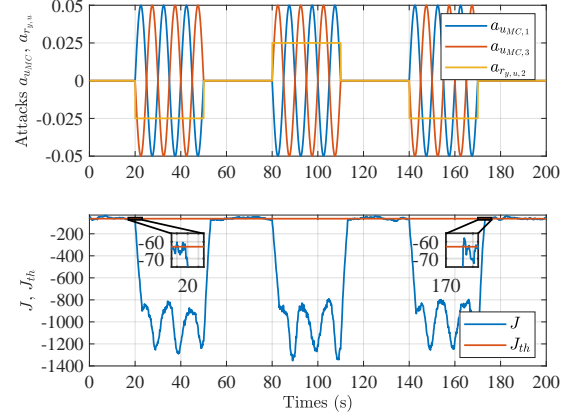


Fig. 7. Detection of attack switching-on and switching-off

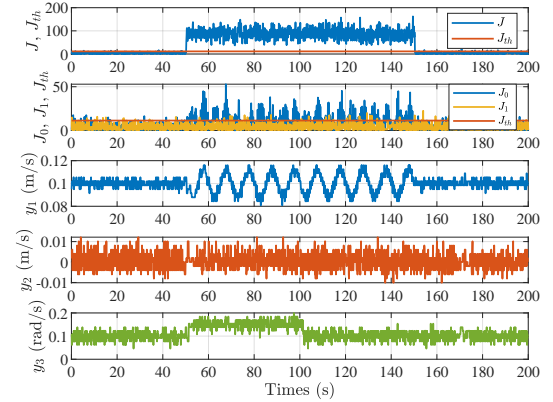


Fig. 8. Detection and resilient control of the traditional CPS configuration

The periodic attacks $a_{u_{MC}}$ and $a_{r_{y,u}}$ are assumed to be launched in [20 s, 170 s], as shown in Fig. 7. According to the experimental results in the second subfigure of Fig. 7, the detector detects the attack switching-on right after 20 s, while the attack switching-off is detected with a delay around 3 s.

E. Comparison study

In this section, we compare our proposed scheme with the traditional CPS configuration (9)-(11). Here, the Kalman filter-based χ^2 detector is utilized for attack detection. The controller in the MC station is implemented as the Youla parameterization-based controller in the observer form. The default Q in (10) is set as $Q = Q_{r,1}$ in (70). For a fair comparison, attacks $a_{u_{MC}}$ and a_y are set the same as those in (34) and (37). Firstly, we would like to compare the attack detection performance. As demonstrated in the first subfigure of Fig. 8, these attacks can be well detected by the χ^2 detector on the MC side. We next consider the cyber-attack (72) with $a_{r_{y,u}} = 0$. The comparison results are shown in the second subfigure of Fig. 8 in which J_0 and J_1 are evaluation functions for our attack detector and the χ^2 detector, respectively. It can be seen that slight input attacks can be detected by our method, while they remain undetectable to the traditional χ^2 detector.

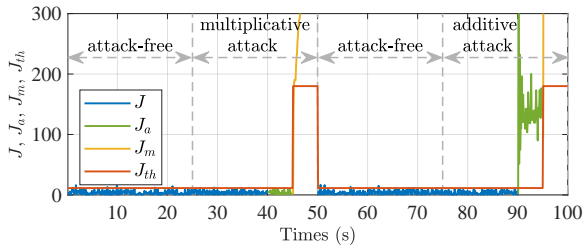


Fig. 9. Detection of additive and multiplicative stealthy attacks

Then, we would like to compare this traditional configuration with our proposed scheme regarding attack resilience performance. In the time interval of $[100\text{ s}, 150\text{ s}]$, the parameter Q is reconfigured by solving the model matching problem as

$$\min_Q \left\| \begin{bmatrix} -\hat{Y} \\ \hat{X} \end{bmatrix} + \begin{bmatrix} M \\ N \end{bmatrix} Q \right\|_{\infty}. \quad (74)$$

The corresponding resilient control performance is illustrated in Fig. 8, which shows the advantage of our resilient control.

F. Detection of additive and multiplicative stealthy attacks

The additive stealthy attacks are designed according to (57). Specifically, attack $a_{u_{MC}}$ is set as

$$a_{u_{MC}}(k) = [a_{u_{MC}}^1(k) \ 0 \ a_{u_{MC}}^3(k)]^T$$

$$a_{u_{MC}}^1(k) = 0.05 \sin(0.2\pi k) + 1, \quad a_{u_{MC}}^3(k) = -0.05 \sin(0.2\pi k) + 1.$$

The attacks $a_{r_{y,u}}$ is generated accordingly. To detect the additive stealthy attacks, the residual $r_{y,u}^a$ is constructed as (69) with the parameter Ψ is set as $\Psi = [5 \times 10^{-2} I \ I]$. Similar as before, a post-filter can be designed for detection purpose and the threshold is set as $J_{th} = 11.3450$.

On the other hand, the multiplicative stealthy attacks are designed according to (59). In this study, we set $\Pi_a = -I$. For detection purpose, the residual $r_{y,u}$ is built according to (63) with the same Ψ . We use a numerical approach to determining the threshold, which returns $J_{th} = 180$. In this study, the detector switching period is set as 25 s, where regular, additive, and multiplicative attack detector take 15 s, 5 s, and 5 s, respectively with J , J_a , and J_m as the associated test statistic. Besides, multiplicative stealthy attacks are lunched in $[25\text{ s}, 50\text{ s}]$, while additive ones are injected in $[75\text{ s}, 100\text{ s}]$. According to Fig. 9, regular attack detector can detect neither the additive nor multiplicative stealthy attacks. The additive and multiplicative stealthy attacks can be detected by their dedicated detectors.

VIII. CONCLUSIONS

This paper is mainly concentrated on the integrated design of detection and resilient control schemes for both the process faults and cyber-attacks for CPSs. To this end, in the first part of this paper, the dynamics of a general type of CPSs under defined types of cyber-attacks have been studied, and the possible impairment of system dynamics have been analyzed. It can be concluded that the cyber-attacks solely affect the image subspace of the process, while the process faults lead to the change exclusively in the image subspace of the controller.

It has been delineated that the capability of the standard observer-based detection and FTC schemes are strongly limited in dealing with the detection and resilient control for cyber-attacks. To handle this issue, an alternative representation of the closed-loop dynamics has been studied, which reveals that i) I/O signal space consists of two complementary subspaces as the image subspaces of the plant and the controller, ii) there exists a one-to-one mapping between I/O signals and the I/O residuals. These observations motivate the second part of this paper to investigate the modified CPS configuration by transmitting $r_{y,u}$ as a fusion of the I/O residuals for both the detection and resilient control purpose.

The further efforts have been dedicated to develop the associated detection schemes for fault detection, cyber-attack detection and resilient FTC. It has been shown that not only the high resilience under cyber-attacks and high fault-tolerance against process faults is ensured, but also the “fail-safe” cyber-security and data privacy are guaranteed with limited online computation and communication effort. To further enhance the security of the proposed CPS configuration, the design schemes of the stealthy attacks against both the tracking behaviour and feedback control performance have been developed from the attacker’s point of view. It is followed by the performance-based detection schemes from the defender’s point of view.

REFERENCES

- [1] S. X. Ding, *Advanced Methods for Fault Diagnosis and Fault-tolerant Control*. Berlin: Springer-Verlag, 2020.
- [2] —, *Data-Driven Design of Fault Diagnosis and Fault-Tolerant Control Systems*. London: Springer-Verlag, 2014.
- [3] L. H. Chiang, E. L. Russell, and R. D. Braatz, *Fault Detection and Diagnosis in Industrial Systems*. London: Springer, 2001.
- [4] R. J. Patton, P. M. Frank, and R. N. C. (Eds.), *Issues of Fault Diagnosis for Dynamic Systems*. London: Springer, 2000.
- [5] H. Alwi, C. Edwards, and C. P. Tan, *Fault Detection and Fault-Tolerant Control Using Sliding Modes*. Springer-Verlag, 2011.
- [6] D. Ding, Q.-L. Han, X. Ge, and J. Wang, “Secure state estimation and control of cyber-physical systems: A survey,” *IEEE Trans. Syst., Man, and Cybern.: Syst.*, vol. 51, no. 1, pp. 176–190, 2021.
- [7] S. Tan, J. M. Guerrero, P. Xie, R. Han, and J. C. Vasquez, “Brief survey on attack detection methods for cyber-physical systems,” *IEEE Systems Journal*, vol. 14, pp. 5329–5339, 2020.
- [8] A. Teixeira, I. Shames, H. Sandberg, and K. H. Johansson, “A secure control framework for resource-limited adversaries,” *Automatica*, vol. 51, pp. 135 – 148, 2015.
- [9] C. Zhou, B. Hu, Y. Shi, Y.-C. Tian, X. Li, and Y. Zhao, “A unified architectural approach for cyberattack-resilient industrial control systems,” *Proceedings of the IEEE*, vol. 109, pp. 517–541, 2021.
- [10] J. Giraldo, D. Urbina, A. Cardenas, J. Valente, M. Faisal, J. Ruths, N. O. Tippenhauer, H. Sandberg, and R. Candell, “A survey of physics-based attack detection in cyber-physical systems,” *ACM Comput. Surv.*, vol. 51, 2018.
- [11] Q. Zhang, K. Liu, Y. Xia, and A. Ma, “Optimal stealthy deception attack against cyber-physical systems,” *IEEE Trans. Cybern.*, vol. 50, no. 9, pp. 3963–3972, 2020.
- [12] S. M. Dibaji, M. Pirani, D. B. Flamholz, A. M. Annaswamy, K. H. Johansson, and A. Chakraborty, “A systems and control perspective of CPS security,” *Annual Reviews in Control*, vol. 47, p. 394–411, 2019.
- [13] Y. Chen, S. Kar, and J. M. F. Moura, “Cyber-physical attacks with control objectives,” *IEEE Trans. Autom. Control*, vol. 63, no. 5, pp. 1418–1425, 2018.
- [14] X.-X. Ren and G. H. Yang, “Kullback–leibler divergence-based optimal stealthy sensor attack against networked linear quadratic gaussian systems,” *IEEE Trans. Cybern.*, vol. 52, no. 11, pp. 11 539–11 548, 2022.
- [15] J. Shang, D. Cheng, J. Zhou, and T. Chen, “Asymmetric vulnerability of measurement and control channels in closed-loop systems,” *IEEE Trans. Contr. Netw. Syst.*, vol. 9, no. 4, pp. 1804–1815, 2022.

- [16] A. M. Mohan, N. Meskin, and H. Mehrjerdi, "A comprehensive review of the cyber-attacks and cyber-security on load frequency control of power systems," *Energies*, vol. 13, 2020.
- [17] S. X. Ding, L. Li, D. Zhao, C. Louen, and T. Liu, "Application of the unified control and detection framework to detecting stealthy integrity cyber-attacks on feedback control systems," *Automatica*, vol. 142, p. 110352, 2022.
- [18] Y. Hu, X. Dai, D. Cui, and Q. Liu, "Anomaly identification for cyber-physical systems subject to replay attacks and sensor faults," *IEEE Trans. Circuits and Systems II: Express Briefs*, 2024, doi: 10.1109/TC-SII.2024.3349777.
- [19] K. Zhang, C. Keliris, T. Parisini, and M. M. Polycarpou, "Identification of sensor replay attacks and physical faults for cyber-physical systems," *IEEE Control Systems Letters*, vol. 6, pp. 1178–1183, 2021.
- [20] M. Ramadan and F. Abdollahi, "An active approach for isolating replay attack from sensor faults," *European Journal of Control*, vol. 69, p. 100725, 2023.
- [21] S. Shen, C. Zhang, R. Chai, L. Dai, S. Chai, and Y. Xia, "Stabilizing nonlinear model predictive control under Denial-of-Service attack via dynamic samples selection," *Automatica*, vol. 164, p. 111591, 2024.
- [22] L. An and G. Yang, "Improved adaptive resilient control against sensor and actuator attacks," *Information Sciences*, vol. 423, pp. 145–156, 2018.
- [23] Z. Ye, D. Zhang, C. Deng, H. Yan, and G. Feng, "Finite-time resilient sliding mode control of nonlinear UMV systems subject to DoS attacks," *Automatica*, vol. 156, p. 111170, 2023.
- [24] M. Segovia-Ferreira, J. Rubio-Hernan, A. Cavalli, and J. Garcia-Alfaro, "A survey on cyber-resilience approaches for cyber-physical systems," vol. 56, no. 8, 2024. [Online]. Available: <https://doi.org/10.1145/3652953>
- [25] T. Sui, Y. Mo, D. Marelli, X. Sun, and M. Fu, "The vulnerability of cyber-physical system under stealthy attacks," *IEEE Trans. Autom. Control*, vol. 66, no. 2, pp. 637–650, 2021.
- [26] J. Zhou, J. Shang, and T. Chen, "Optimal deception attacks on remote state estimators equipped with interval anomaly detectors," *Automatica*, vol. 148, p. 110723, 2023.
- [27] J. Qin, M. Li, L. Shi, and X. Yu, "Optimal denial-of-service attack scheduling with energy constraint over packet-dropping networks," *IEEE Trans. Autom. Control*, vol. 63, no. 6, pp. 1648–1663, 2018.
- [28] L. An and G. H. Yang, "Data-driven coordinated attack policy design based on adaptive \mathcal{L}_2 -gain optimal theory," *IEEE Trans. Autom. Control*, vol. 63, no. 6, pp. 1850–1857, 2018.
- [29] Z. Guo, D. Shi, K. H. Johansson, and L. Shi, "Worst-case stealthy innovation-based linear attack on remote state estimation," *Automatica*, vol. 89, pp. 117–124, 2018.
- [30] X. Ren, J. Wu, S. Dey, and L. Shi, "Attack allocation on remote state estimation in multi-systems: Structure results and asymptotic solution," *Automatica*, vol. 87, pp. 184–194, 2018.
- [31] G. Wu, J. Sun, and J. Chen, "Optimal data injection attacks in cyber-physical systems," *IEEE Trans. Cybern.*, vol. 48, no. 12, pp. 3302–3312, 2018.
- [32] C. Fang, Y. Qi, J. Chen, R. Tan, and W. Zheng, "Stealthy actuator signal attacks in stochastic control systems: Performance and limitations," *IEEE Trans. Autom. Control*, vol. 65, no. 9, pp. 3927–3934, 2020.
- [33] L. Guo, H. Yu, and F. Hao, "Optimal allocation of false data injection attacks for networked control systems with two communication channels," *IEEE Trans. Control Netw. Syst.*, vol. 8, no. 1, pp. 2–14, 2021.
- [34] Z. Zhao, Y. Huang, Z. Zhen, and Y. Li, "Data-driven false data-injection attack design and detection in cyber-physical systems," *IEEE Trans. Cybern.*, vol. 51, no. 12, pp. 6179–6187, 2021.
- [35] K. Jin and D. Ye, "Optimal innovation-based stealthy attacks in networked LQG systems with attack cost," *IEEE Trans. Cybern.*, vol. 54, pp. 787–796, 2024.
- [36] J. Shang, D. Cheng, J. Zhou, and T. Chen, "Asymmetric vulnerability of measurement and control channels in closed-loop systems," *IEEE Trans. Contr. Net. Syst.*, vol. 9, pp. 1804–1815, 2022.
- [37] Q. Zhang, K. Liu, A. M. H. Teixeira, Y. Li, S. Chai, and Y. Xia, "On online kullback-leibler divergence-based stealthy attack against cyber-physical systems," *IEEE Trans. Autom. Control*, vol. 68, pp. 3672–3679, 2023.
- [38] A. Lu and G.-H. Yang, "False data injection attacks against state estimation without knowledge of estimators," *IEEE Trans. Autom. Control*, vol. 67, no. 9, pp. 4529–4540, 2022.
- [39] Y. Mo and B. Sinopoli, "On the performance degradation of cyber-physical systems under stealthy integrity attacks," *IEEE Trans. Autom. Control*, vol. 61, pp. 2618–2624, 2016.
- [40] K. Zhou, J. Doyle, and K. Glover, *Robust and Optimal Control*. Upper Saddle River, New Jersey: Prentice-Hall, 1996.
- [41] P. Griffioen, S. Weerakkody, and B. Sinopoli, "A moving target defense for securing cyber-physical systems," *IEEE Trans. Autom. Control*, vol. 66, pp. 2016–2031, 2021.
- [42] T. Li, Z. Wang, L. Zou, B. Chen, and L. Yu, "A dynamic encryption–decryption scheme for replay attack detection in cyber–physical systems," *Automatica*, vol. 151, p. 110926, 2023.
- [43] D. Zhou, Y. Zhao, Z. Wang, X. He, and M. Gao, "Review on diagnosis techniques for intermittent faults in dynamic systems," *IEEE Trans. on Indus. Electronics*, vol. 67, pp. 2337 – 2347, 2020.
- [44] R. S. Smith, "Covert misappropriation of networked control systems: Presenting a feedback structure," *IEEE Control Systems Magazine*, vol. 35, pp. 82–92, 2015.
- [45] Q. Zhang, K. Liu, A. M. H. Teixeira, Y. Li, S. Chai, and Y. Xia, "An online kullback–leibler divergence-based stealthy attack against cyber-physical systems," *IEEE Trans. Autom. Control*, vol. 68, no. 6, pp. 3672–3679, 2023.
- [46] H. Liu, Y. Ni, L. Xie, and K. H. Johansson, "How vulnerable is innovation-based remote state estimation: Fundamental limits under linear attacks," *Automatica*, vol. 136, p. 110079, 2022.
- [47] X.-X. Ren, G.-H. Yang, and X.-G. Zhang, "Optimal stealthy attack with historical data on cyber–physical systems," *Automatica*, vol. 151, p. 110895, 2023.
- [48] K. Jin and D. Ye, "Optimal innovation-based stealthy attacks in networked lqg systems with attack cost," *IEEE Trans. Cybern.*, vol. 54, no. 2, pp. 787–796, 2024.